AD-A153 066 A FRACTURE MECHANICS AND CRACK PROPAGATION APPROACH TO THE STUDY OF OVERC..(U) CASE INST OF TECH CLEVELAND OH DEPT OF CIVIL ENGINEERING A S SAADA ET AL. FEB 85 1/1

UNCLASSIFIED SFRAC-1 ARO-18871.2-GS DAAG29-83-K-0010 F/G 8/13 NL

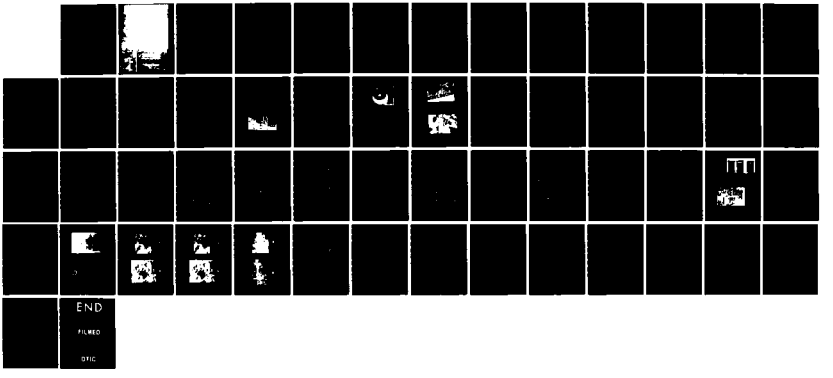

END

FILMED

DTIC

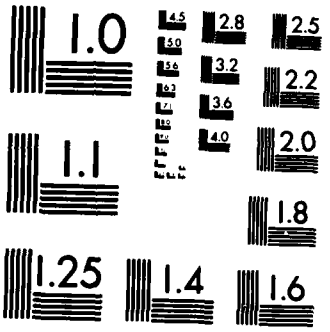

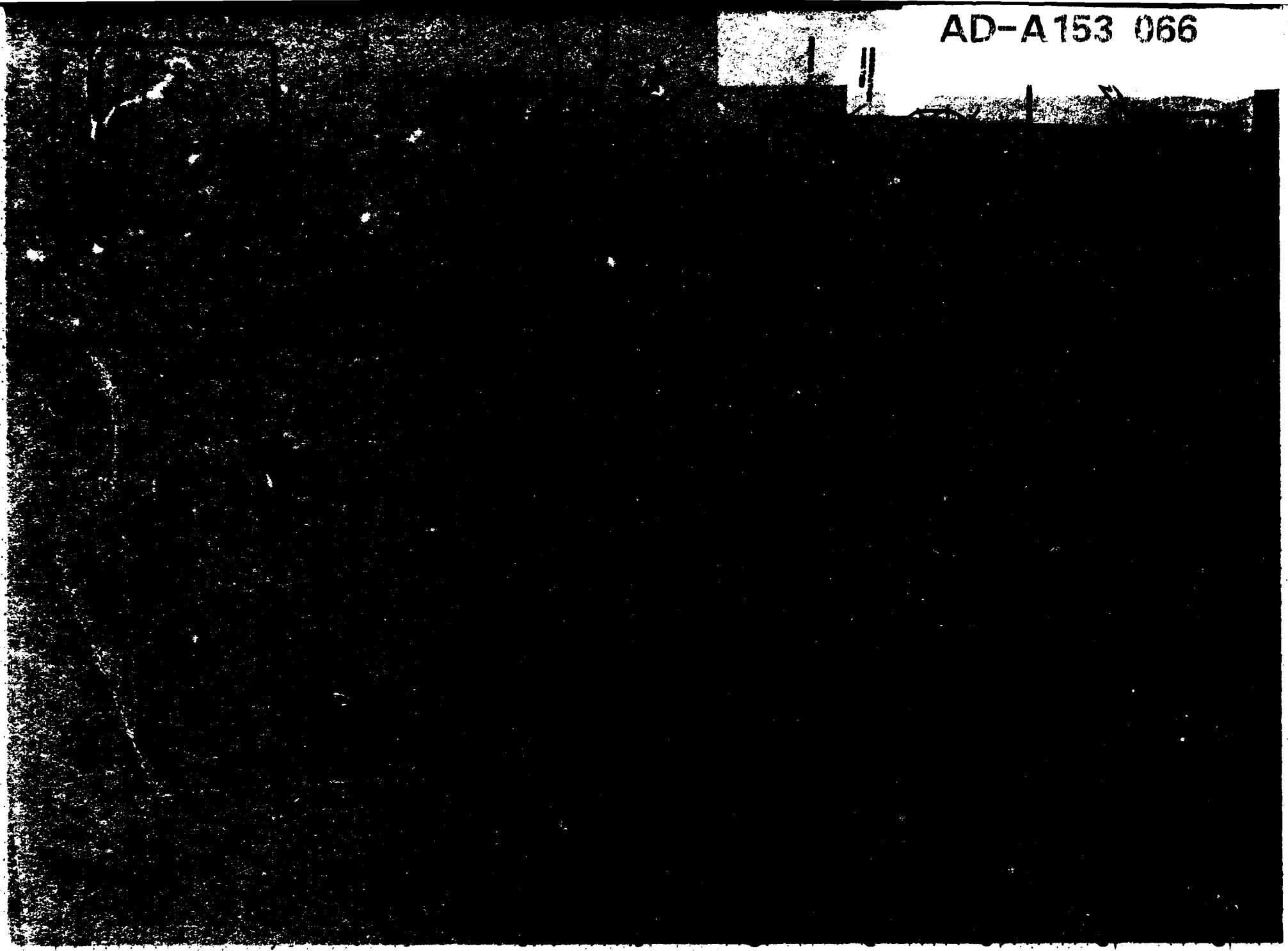

UNCLASSIFIED

SECURITY CLASSIFICATION OF THIS PAGE (When Data Entered)

REPORT DOCUMENTATION PAGE		READ INSTRUCTIONS BEFORE COMPLETING FORM
1. REPORT NUMBER ARO 18871.2-GS	2. GOVT ACCESSION NO. N/A	3. RECIPIENT'S CATALOG NUMBER N/A
4. TITLE (and Subtitle) A FRACTURE MECHANICS AND CRACK PROPAGATION APPROACH TO THE STUDY OF OVERCONSOLIDATED CLAY		5. TYPE OF REPORT & PERIOD COVERED Final Technical Report 12/1/82 - 11/30/84 6. PERFORMING ORG. REPORT NUMBER
7. AUTHOR(s) Prof. Adel S. Saada Prof. Alexander Chudnovsky		8. CONTRACT OR GRANT NUMBER(s) DAAG29-83-K-0010
9. PERFORMING ORGANIZATION NAME AND ADDRESS Dept. of Civil Engineering Case Western Reserve Universit- Cleveland, Ohio 44106		10. PROGRAM ELEMENT, PROJECT, TASK AREA & WORK UNIT NUMBERS
11. CONTROLLING OFFICE NAME AND ADDRESS U. S. Army Research Office Post Office Box 12211 Research Triangle Park, NC 27709		12. REPORT DATE February, 1985 13. NUMBER OF PAGES
14. MONITORING AGENCY NAME & ADDRESS(if different from Controlling Office)		15. SECURITY CLASS. (of this report) Unclassified 15a. DECLASSIFICATION/DOWNGRADING SCHEDULE

16. DISTRIBUTION STATEMENT (of this Report)

Approved for public release; distribution unlimited.

ELECTE
MAY 1 1985
A

17. DISTRIBUTION STATEMENT (of the abstract entered in Block 20, if different from Report)

NA

18. SUPPLEMENTARY NOTES

The view, opinions, and/or findings contained in this report are those of the author(s) and should not be construed as an official Department of the Army position, policy, or decision, unless so designated by other documentation.

19. KEY WORDS (Continue on reverse side if necessary and identify by block number)

Fracture ~~Mode~~	Damage Zone
Overconsolidated Clay	Irreversible Thermodynamics
Stress Intensity Factors	Kinetics
Crack Propagation	Stability

Coal Mechanics

20. ABSTRACT (Continue on reverse side if necessary and identify by block number)

Ideas and concepts about fracture and crack propagation in overconsolidated clays have been part of geotechnical engineering thinking for years. Those concepts, however, were never formalized, primarily due to the overwhelming hold plasticity theory had an still has on the profession. To the knowledge of the authors this is the first time the mechanical behavior of stiff clays is studied and analyzed through the discipline of fracture mechanics.

(over)

DD FORM 1 JAN 73 1473 EDITION OF 1 NOV 65 IS OBSOLETE

UNCLASSIFIED

SECURITY CLASSIFICATION OF THIS PAGE (When Data Entered)

A test is developed to determine the critical stress intensity factor K_{IC} for the opening mode. The specimen with the configuration of a hollow disk and a notch cut in its internal surface is fatigued under cyclic internal pressure, then failed to determine the pattern of crack propagation. The critical length of the crack is ~~then~~ used to determine K_{IC} for various degrees of overconsolidation. While overconsolidation leads to an increase in strength, ~~it was found that~~ it resulted in a noticeable decrease in the value of K_{IC}.

A second test was developed to determine the critical stress intensity factor K_{IIC} for the shearing mode. ~~It is noteworthy that~~ this is the first time a non-ambiguous mode II fracture has been obtained for any material. The specimen with the configuration of a thin long hollow cylinder with a notch cut into it, is subjected to hydrostatic pressure and pure torsion. Here too, the knowledge of the critical crack length and shearing stress allows one to get K_{IIC} for a large spectrum of overconsolidation ratios. Here, however, the influence of overconsolidation on K_{IIC} was much smaller than that observed on K_{IC}.

Most intriguing are the observed damage zones which have very little if anything to do with the predictions of plasticity theory. A honey combed network of fissures was observed enclosing undamaged material with localized discontinuities emanating from the tip of the crack. Here damage zone theory rather than plasticity is the most promising tool in the process of understanding the deformation and failure of fissured clays.

K_{IC} and K_{IIC} characterize catastrophic failure and do not describe the phenomenon of slow crack propagation. The kinetics of crack propagation for mode I was studied by direct surface observation. Those observations were compared to crack lengths calculated from crack opening displacement measurements. The relation between the rate of crack propagation with respect to the number of cycles, and the energy release rate which was deduced, is at the core of the development of constitutive equations for crack propagation; provided it is verified in further experiments on different clays.

A thermodynamic criterion of stability is applied to the stability of an infinite slope with a crack parallel to the surface.

FORWARD

The study reported herein was made by the faculty and students of Case Western Reserve University (CWRU) during the period 1 December, 1982 through 30 December, 1984. The investigation was sponsored by the U.S. Army Research Office, under Research Agreement No. DAAG29-83-K-0010 and the supervision of Dr. Steven J. Mock of the Geosciences Division. The Co-Principal Investigators were Professors Adel S. Saada and Alexander Chudnovsky, Graduate Students M. Kennedy and M. Sharaf participated in this investigation as part of their Master's degree requirements.

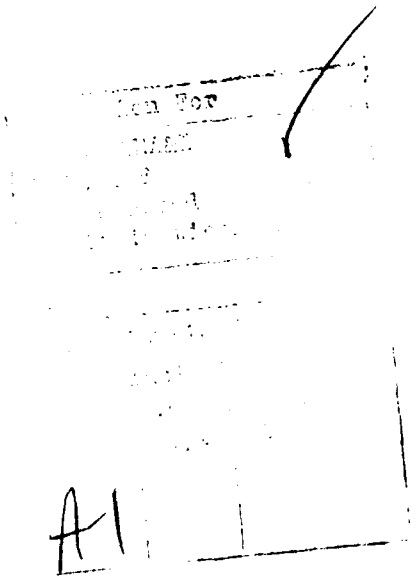

CONTENTS

LIST OF ILLUSTRATIONS

PART I: INTRODUCTION

Ia - Soil Mechanics and Fracture Mechanics - A Review of Some Relevant Work

Cracks are very often observed in stiff clays. Some appear during a shrinkage process; some appear during an expansion process; and some are initiated by high levels of stress concentration at low nominal stress levels. Once a crack has been initiated subsequent propagation may follow any of the three modes shown in Fig. 1. Mode I, the opening mode, is of importance in hydraulic fracturing and modes II and III, the shearing modes, are of interest in all problems involving sliding.

Ideas and concepts about fracture and crack propagation have been in the back of the mind of geotechnical engineering researchers for years. Often the terminology is different from that used by classical fracture mechanicians, but the problems are common. The geotechnical engineering profession is quite familiar with stiff fissured or jointed clays where the discontinuities, in contrast to the Griffith cracks, are found on a macroscopic scale (Fig. 2). The possible geological processes that may lead to the formation of fissures has been discussed by Fookes [7]. A preliminary classification of different types of discontinuities which constitute planes of weakness has been given by Skempton and Petley [15] and Skemption, Schuster and Petley [16]. The importance of size effect on the undrained strength of stiff fissured clay was demonstrated by Bishop and Little [2] who showed that the strength of London clay determined by in-situ shear box testing on a 2 ft. by 2 ft. square sample is only 55 percent of that given by laboratory unconsolidated undrained triaxial tests on 1.5 in. diameter samples. Similar strength decrease was found for blue

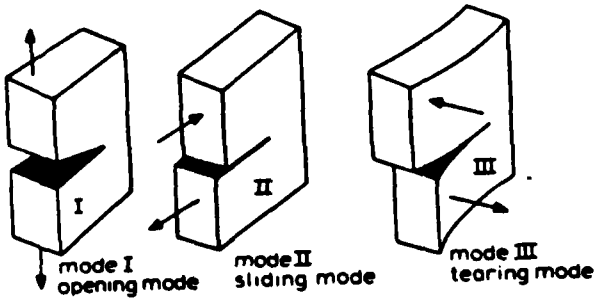

FIG. 1 Fracture Modes

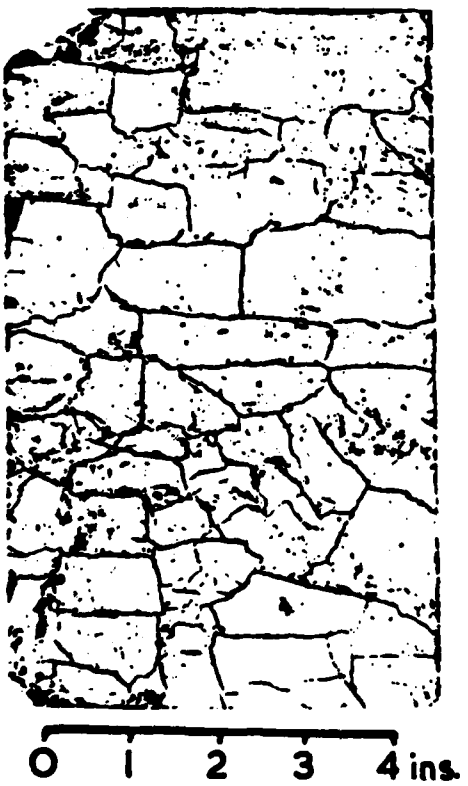

FIG. 2 Vertical Section Through Typical Fissured Clay

London clay by Simons [13]. For a glacio-lacustrine clay north of lake Erie, Lo, adams and Seychuk [19] found that the size effect was more pronounced. The phenomenon is therefore, not only a mathematical probability, but a physical reality of no infrequent occurence. The remarkable work of Lo [9] on the operational strength of fissured clay has in it most of the elements on which classical fracture mechanics rests.

A characteristics common to "most" stiff clays is that they are overconsolidated and therefore they have the capacity of decreasing their shearing strength with increasing deformation. Deformation is time dependent and, as pointed out by Morgenstern [10], one has to distinguish betwen two aspects of the time dependent behavior of soils. These are creep and progressive failure. A soil exhibiting creep at a given stress level will still be able to sustain a higher stress level although possibly with a higher strain rate. The best documented evidence for creep in soils is secondary consolidation and field evidence shows that secondary consolidation in stiff clays can be substantial and depend upon the history of loading [4]. Progressive failure relates to the fact that the available shearing resistance of a soil mass can be between the peak and the residual value. The strength can be attacked in various ways giving rise to displacements which vary with time. When the shearing strength drops below the shearing stress, catastrophic movement can ensue. Both creep and progressive failure are dependent upon the loading path.

In his Terzaghi lecture Bjerrum [3] states that in order to start a progressive failure there must be a discontinuity somewhere in the clay mass where failure can be initiated and the deformations required for further development can be produced. Stress concentrations, in other words

local high shearing stresses exceeding the peak are given as a prerequisite for the development of a continuous failure surface by progressive failure. The more overconsolidated the clay, the greater its content of recoverable strain energy and the greater the danger of progressive failure. Bishop [1] defined brittle clays by means of a brittleness parameter defined by (Fig. 3)

$$I_B = \frac{\tau_f - \tau_r}{\tau_f} \%$$

which for overconsolidated soils varies with stress. He also suggested that brittleness may be considered in terms of the additional energy required to make the shear failure progress from the peak to the residual state (Fig. 3). This is represented by the shaded area E_f. If the sample had shown no drop in strength after the peak, the work done would have been represented by E_p. The difference between these areas expressed as a ratio of E_p may be a useful measure of brittleness also. It was called the rupture index (Fig. 3):

$$\text{Rupture Index} = \frac{E_p - E_f}{E_p}$$

Bishop cautioned against evaluating any parameter based on the shape of the stress strain curve, particularlily after the peak, because of the tendency for failure to develop in a single thin shear zone in many samples which show marked dilatancy or marked structural breakdown or shear.

The mechanism of propagation of a shear surface in a fissured clay may well prove to involve concepts similar to those put forward by Griffith. These include energy absorbed in forming the surface and released by relieving the stresses in the locally highly stressed material adjacent to it.

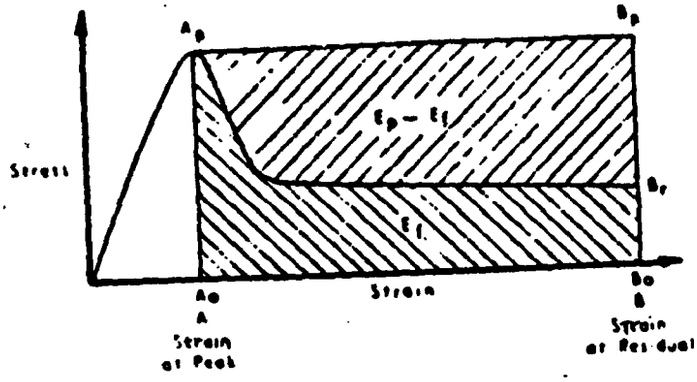

E_p = Work done in moving from A to B if there is no drop in strength (area $A_o A_p B_p B_o$)

E_f = Actual work done in moving from A to B (area $A_o A_p B_r B_c$)

$$\text{Rupture index} = \frac{E_p - E_f}{E_p} = \frac{(\text{Area } A_p B_p B_r)}{(\text{Area } A_o A_p B_p B_o)}$$

Fig. 3 An Energy Parameter for Brittle Soils

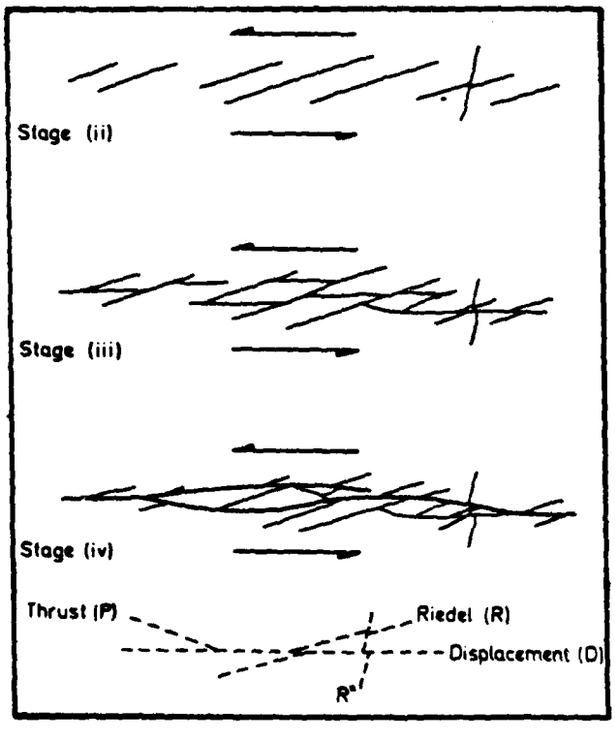

FIG. 4 Successive Stages in the Development of Shear Zones

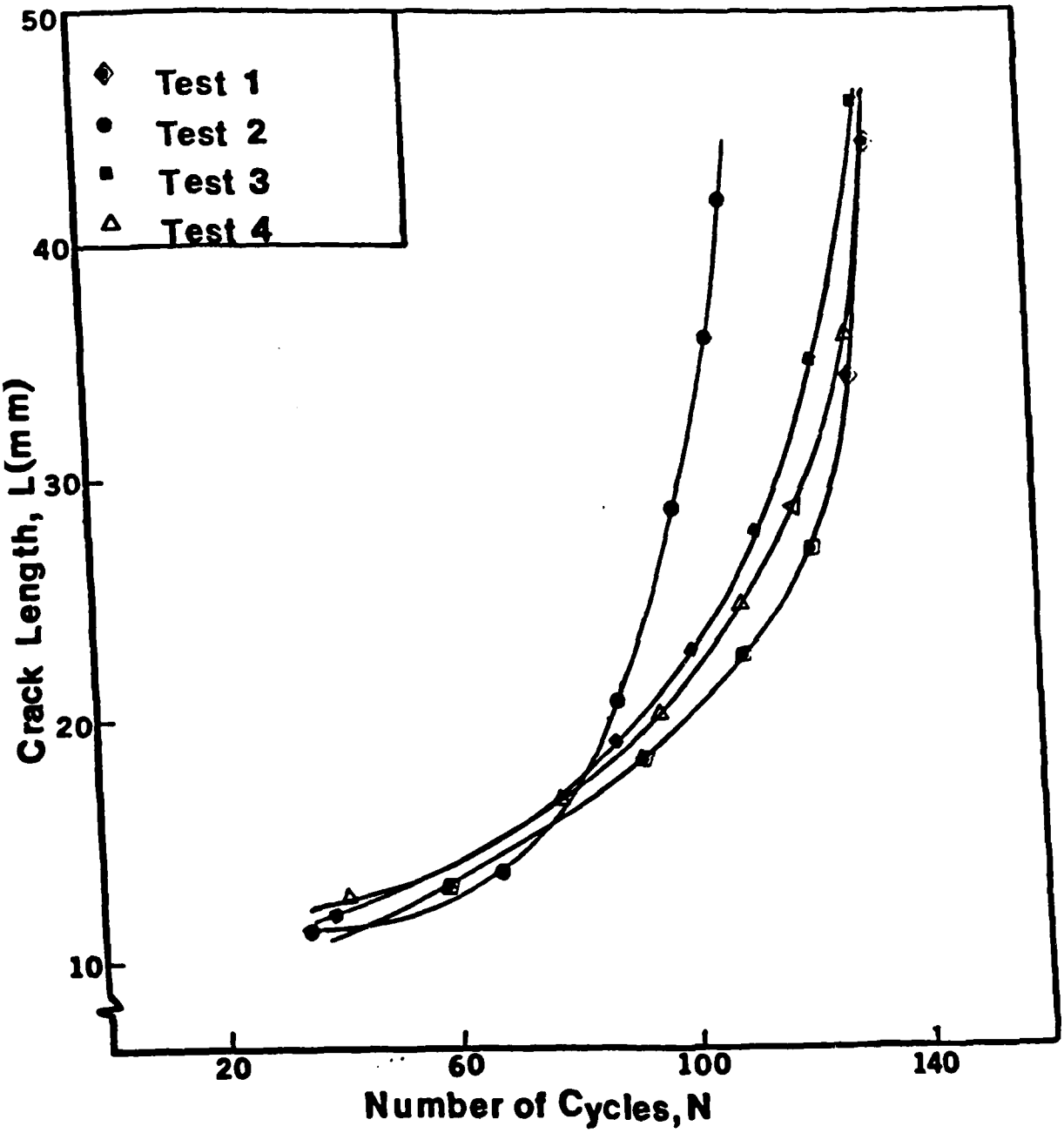

FIG. 15 Crack Length Versus Number of Cycles for Four Tests

IIc - Kinetics of Crack Propagation

To study the kinetics of crack propagation four tests were conducted during which the crack length was measured as the number of internal pressure cycles increased. Fig. 15 shows the results of those tests. Average values are plotted in Fig. 16 together with a measure of the amount of scatter. As previously indicated the crack length is measured on the face of the disk with a follower attached to an LVDT. There is no guarantee that this crack length extends all the way across the material. Thus, an alternate method for recording the crack length was sought. This method is based on a simple relation between the crack length and the crack opening δ at a certain point. According to Castigliano's second theorem, for a linearly elastic material, the displacement δ caused by a load Q is given by

$$\delta = \frac{\partial U}{\partial Q} = - \frac{\partial \Pi}{\partial Q} \tag{6}$$

where U is the strain energy of the solid and Π the potential energy.

Let us consider the disk shown in Fig. 17. The potential energy can be expressed as:

$$\Pi = \Pi_{\text{no crack}} - \int_0^{\ell} \frac{\partial \Pi}{\partial Q} \, d\ell. \tag{7}$$

The derivative $- \frac{\partial \Pi}{\partial \ell}$ is the energy release rate J_1 for linear elasticity and can be expressed in terms of the stress intensity factor:

$$- \frac{\partial \Pi}{\partial \ell} = \frac{(1 - \nu^2)}{E} K_I^2 \tag{8}$$

To compute the crack opening δ at a distance c from the inner face of the

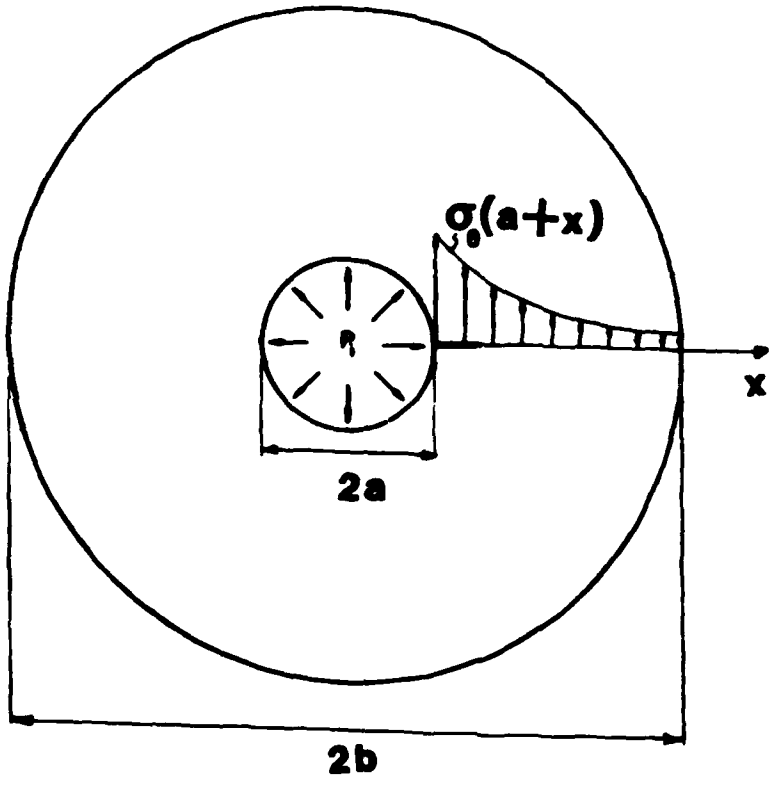

FIG. 13 Elastic Stress Distribution in a Hollow Disk

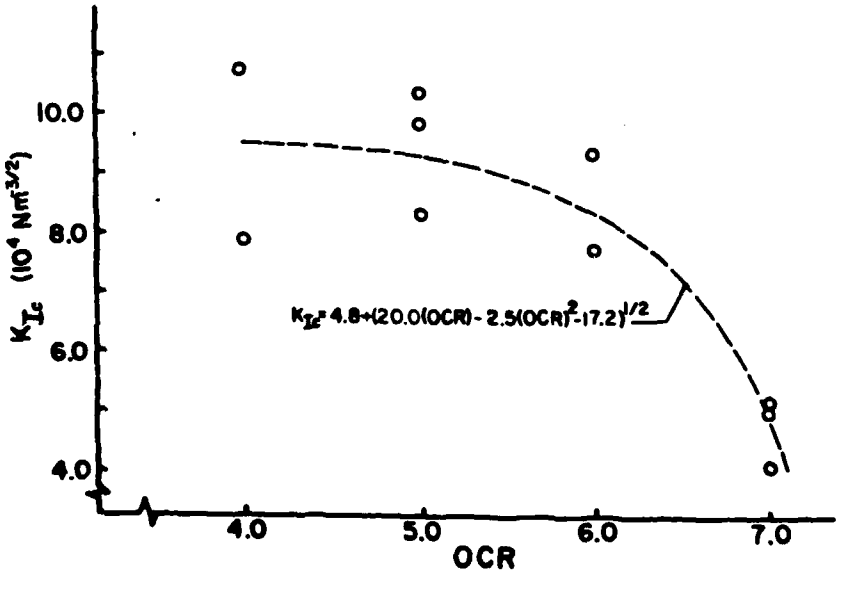

FIG. 14 K_{IC} for Overconsolidated Clay

Green's function $G_K(x)$ for the hollow disk with a crack emanating from the hole is not known. As a first approximation use was made of Green's function for the stress intensity factor in the strip shown in Fig. 12:

$$G_K = \frac{2}{\sqrt{\pi \ell}} F(\frac{x}{\ell}, \frac{\ell}{w}) \tag{3}$$

where $F(\frac{x}{\ell}, \frac{\ell}{w})$ is a geometric correction factor given in reference 17 page 2-27. To apply Eq. 3 to the hollow disk we set (b-a) equal to W. b and a are the outer and inner radii of the disk. The elastic stress distribution along a radius in a hollow disk subjected to internal pressure is given by (Fig.13).

$$\sigma_\theta(a + x) = \frac{pa^2}{b^2 - a^2} [1 + (\frac{b}{a + x})^2] \tag{4}$$

Using the superposition principle and equations 2, 3 and 4, the stress intensity K_I for a hollow disk with a crack emanating from the hole is

$$K_I = \frac{2Pa^3}{\sqrt{\pi \ell}\ (b^2 - a^2)} \int_0^{\ell} F(\frac{x}{\ell}, \frac{\ell}{b - a}) [1 + (\frac{b}{a + x})^2] dx \tag{5}$$

Numerical integration of Eq. 5 leads to the curve shown in Fig. 12. If ℓ and p are replaced by their critical value ℓ_c and P_c and substituted in Eq. 5, the critical value K_{IC} of the stress intensity factor is obtained. For the tests conducted in this investigation, this value as a function of the overconsolidation ratio is shown in Fig. 1A. K_{IC} is a basic parameter to be used in design when failures such as those occurring during hydraulic fracturing are studied.

Damage zone propagation studies are presently in progress to clarify the dependence of K_{IC} on the preconsolidation pressure.

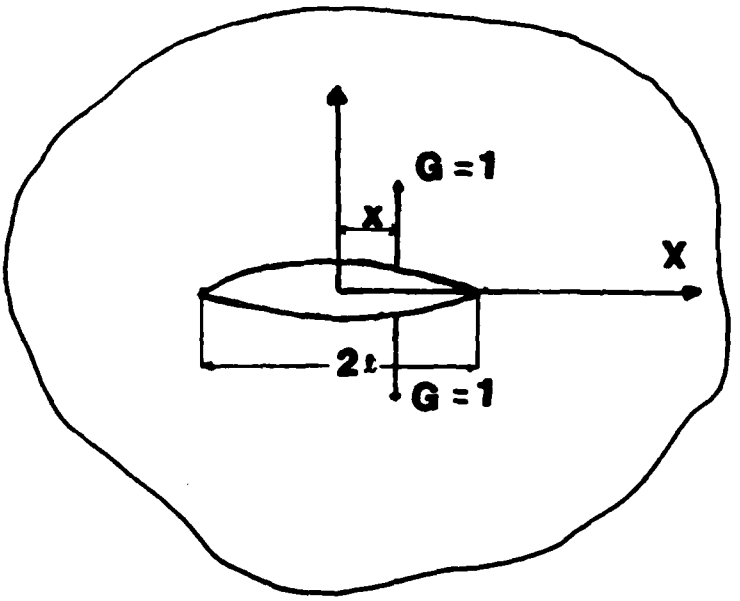

FIG. 11 Calculation of K_{IC}

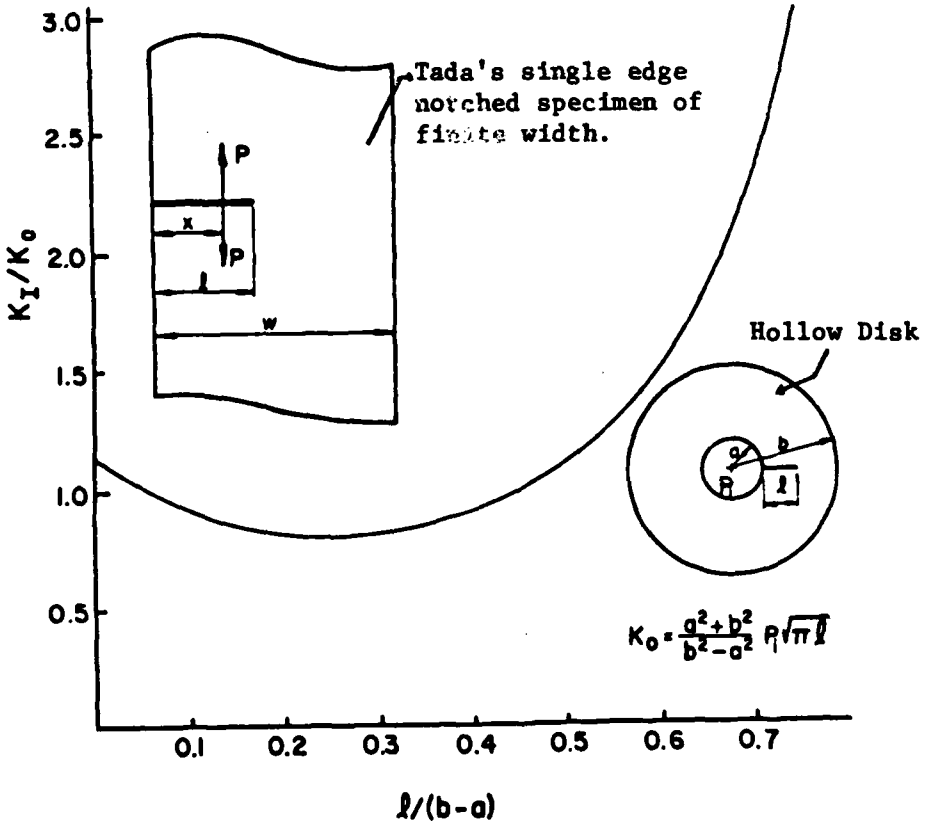

FIG. 12 Determination of K_I for a Hollow Disk

overconsolidation ratio were mounted in the testing fixture as shown in Fig. 8 and sinusoidally varying air pressure sent through the air inlet. Under cyclic pressure the crack propagates in a stable manner as long as the pressure is moderate and the crack length below the critical. The crack was allowed to propagate half way through thickness to allow for the study of damage zones. Crack propagation was followed with a pointer attached to an LVDT. The crack opening displacement (COD) was measured with a transducer mounted on the specimen. The cyclic loading was then stopped and a sudden high pressure was applied inside the membrane which caused failure in a very short time. An X-Y plotter gave a graph of the inside pressure versus the COD. The maximum pressure is the critical pressure. The critical length was obtained from the examination of the fracture surface.

Fig. 9 shows the whole apparatus designed and built for this purpose. Fig. 10 shows the details of the micrometer driven pointer following the crack propagation.

IIb - Calculation of K_{IC}

The most general and elegant way to calculate K_I is through the use of Green's function. Let $G_K(x)$ be Green's function for the stress intensity factor for a given sample geometry; i.e., the expression for the stress intensity factor K_I caused by the unit double forces applied at the point x (Fig. 11):

$$K_I = G_K(x) \tag{1}$$

Then for an arbitrarily distributed traction $\sigma(x)$ normal to the crack's edges, the stress intensity factor is given by,

$$K_I = \int_{-\ell}^{+\ell} G_K(x)\ \sigma(x)dx \tag{2}$$

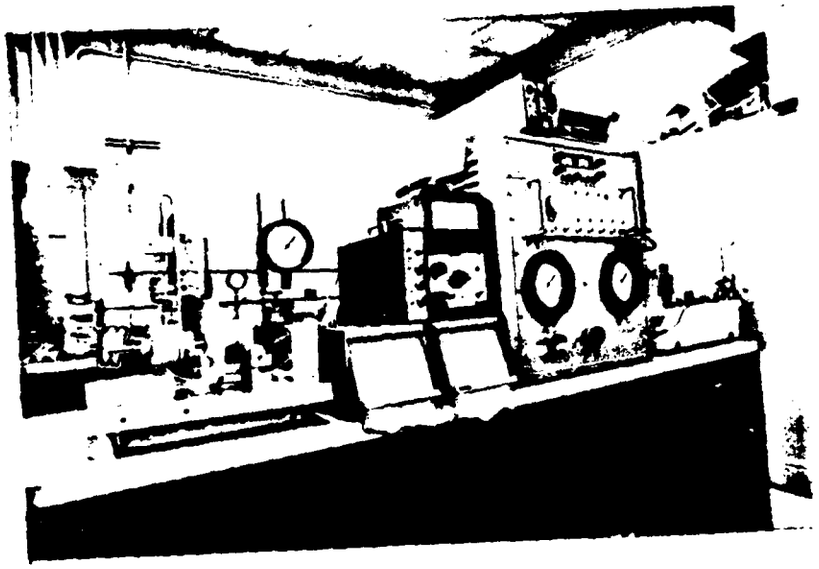

FIG. 9 Mode I Test Set Up

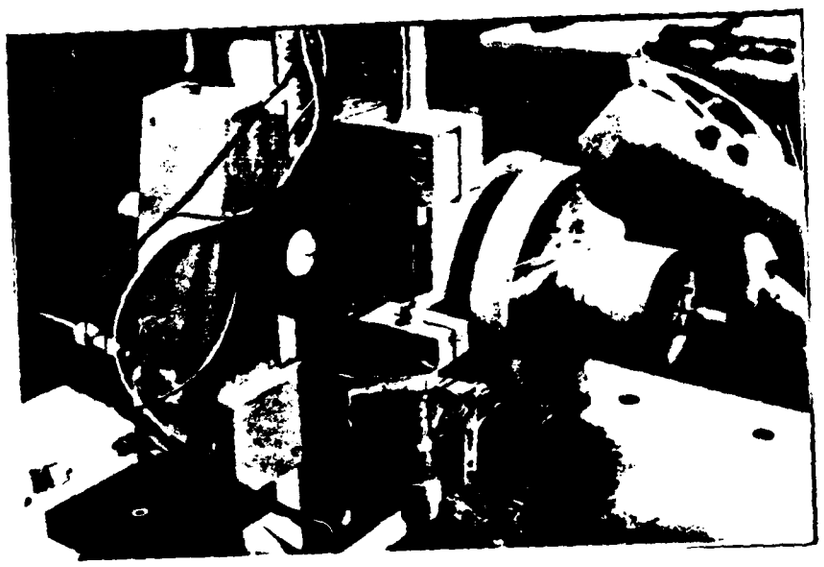

FIG. 10 Crack Propagation and COD Measurements

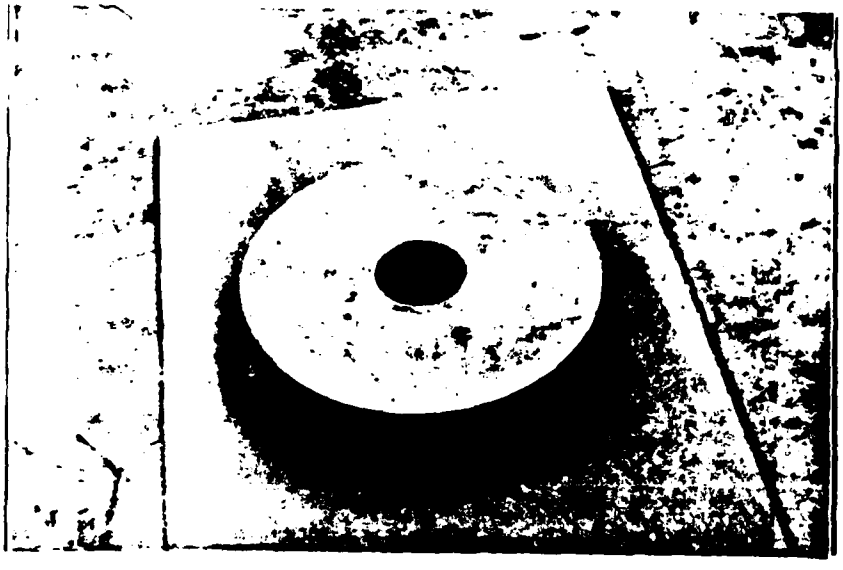

FIG. 7 Specimen for Mode I Test

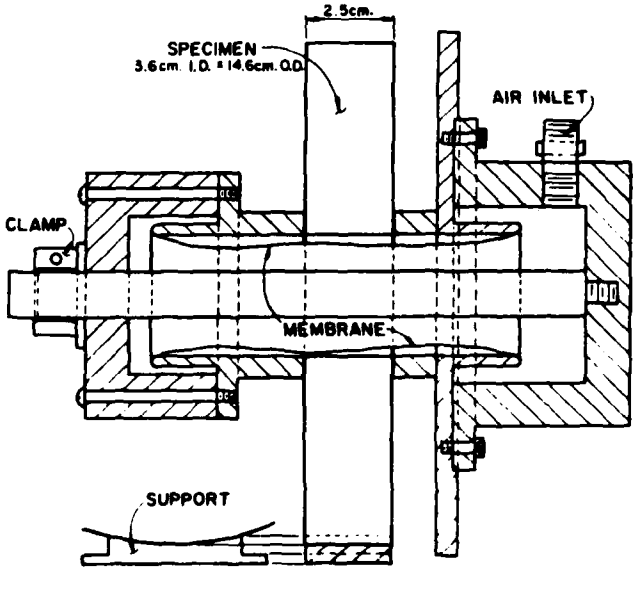

FIG. 8 Mode I Test Fixture

PART II: DETERMINATION OF THE CRITICAL VALUE OF THE STRESS INTENSITY FACTOR K_{IC} FOR MODE I FRACTURE

Fracture Modes I and II are respectively distinguished by symmetry and antisymmetry of stress, strain and displacement fields with respect to the crack plane. For Mode I fracture the sample configuration used is that of a hollow disk with a precut notch or stress concentration cut in the inside edge. Static or dynamic pressure is applied to the inner surface through a rubber membrane.

For linear elastic media, the stress intensity factor K_I is uniquely defined by the stress and the length. Thus, its critical value K_{IC} can be obtained once the value of the critical stress and that of the critical crack length at which unstable fracture takes place are known.

IIa - Sample Preparation and Testing Equipment

Kaolinite clay with liquid and plastic limits of 56.3 percent and 37.5 percent respectively was mixed with deaired distilled water at twice the liquid limit. The slurry was consolidated in a large metal consolidometer under a series of pressures namely 414, 517, 620 and 723 kPa to provide a range of overconsolidation ratios. After equilibrium was reached the clay was allowed to rebound under atmospheric pressure leading to overconsolidation ratios of 4, 5.1, 6.1 and 7.1 respectively. Fig. 6 shows the consolidometer set-up.

The blocks of clay were sliced horizontally to yield specimens 25mm thick. A simple rig was used to punch a 35.6mm hole at the center of the discs and to cut a radial notch 10mm deep (Fig. 7). They were covered with silicone oil wrapped and stored in a fog room. The specimens with a given

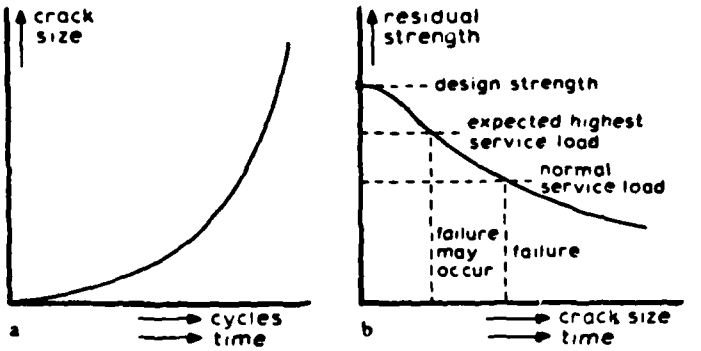

FIG. 5 Crack Growth and Residual Strength curves

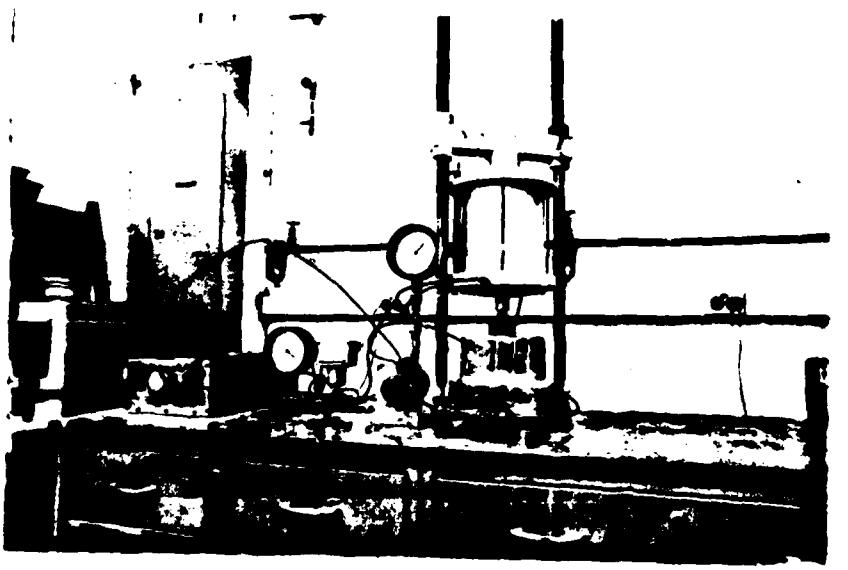

FIG. 6 Sample Preparation

their density and their statistical distribution in the material.

Ic - Goals of the Present Study

Following a path similiar to that taken for other materials, this study seeks to develop standard tests for the determination of K_I and K_{II} for stiff clays. Zones of microcracking are studied as well as the kinetics of crack propagation. This and future investigations well hopefully lead to realistic constitutive relations and lay a foundation for better understanding the behavior of stiff clays under static and dynamic loading.

very small peak. High stress concentrations or large strains are needed to initiate cracks in such clays. Often, however, inclusions such as coarse particles from stress concentrators for cracks to start and propagate.

Due to the presence of a crack the strength of the soil is decreased. As the size of the crack increases with time additional degradation of the strength takes place (Fig. 5). After a certain time it becomes so low that the soil cannot withstand accidental high loads that may occur in service. From this moment on the soil is liable to fail. On the other hand, if accidental high loads do not occur, cracks may continue to grow with time until the strength falls below the service load. With respect to Fig. 5, fracture mechanics should help answer the following questions:

1 - What is the strength as a function of the crack size?

2 - What size of crack can be tolerated at the expected service stresses (static or dyanmic)? And what is the critical crack size?

3 - Under a given state of loading, how long does it take for a crack to grow from a certain initial size to the critical size?

4 - How do cracks coalesce and ultimately reduce the strength to its residual value?

Many theories which have been found satisfactory for both brittle and ductile materials have never been tried for clays. The aim of this research is to examine the mechanical behavior of clay from the point of view of fracture mechanics. Since failure generally appears in the form of a surface, one has to start by studying the single crack and its propagation, followed by the coalescence of cracks; a topic which obviously involves

presently the subject of some research and may become another useful tool in the geotechnical engineering arsenal. Some results suggest that the mechanism involved is that of a tensile failure resulting from water pressure acting on a crack in a soil medium. A discontinuity is needed and the soil at the tip of the crack deforms plastically.

More recently researchers have turned their attention to the behavior of clays under large cyclic loadings. Under such loadings cracks can be initiated as a result of plastic deformations. Even if the nominal stresses are well below the yield limit, locally the stresses may be above yield due to stress concentrations such as those occurring in simple shear devices. Cracks can coalesce after a number of cycles leading to fatigue fracture.

1b - Some Questions to be Answered by Fracture Mechanics

Under stress clays seem to have in them the capability of responding as elastic, viscous or plastic materials. It all depends on the level and the rate at which the stresses are applied. They can be in a brittle state or in a plastic state; they can be intact or fissured; they can be insensitive; they can be strain hardening or strain softening. High overconsolidation ratios lead to clays which develop fissures upon rebound, and such fissures can be visible to the naked eye; they have a residual strength much lower than the peak. Moderate overconsolidation ratios result in clays which "may" have in them flaws or micro-cracks invisible to the naked eye, but whose presence expresses itself through the existence of a peak and a residual strength; and through an influence of the size of the test specimen on the strength. Low overconsolidation ratios result in clays whose behavior is of the strain hardening type or at best presents a

Skempton [14] recognized five stages in the shearing deformation of a stiff clay. The first one before the peak is one of continuous non-homogeneous strain. In the second which occurs at or just before the peak Riedel shears are formed (Fig. 4). They lie en echelon at an inclination usually between 10 to 30 degrees to the direction of general movement (the D axis) and conjugate shears R* are sometimes seen. With further movement a third stage is soon reached at which slip along the Riedel shear is no longer kinematically possible and the clay is compelled to develop new slip surfaces parallel or subparallel to the D axis. These are the displacement shears. With greater movement the displacement shears extend and eventually in the fourth stage some of them link up to form a slip surface. This surface is undulating since the shears involved were not originally all in line. Thrust shears typically inclined at about 160° to the D axis also tend to develop in the third and fourth stages. In the fifth stage the slip surface undergoes appreciable flattening as a result of still greater movements. Once a slip surface has formed subsequent movements are mostly concentrated along it; and large displacements can then take place without a fundamental change in the pattern of shears. the development of shear is accompanied by particle orientation. Morgenstern and Tchalenko [11] and Yong and Warkentin [18] have shown that the slip surface consists of a thin band in which the particles are strongly oriented more or less in the direction of the movement. A flattened slip surface must possess the minimum shear resistance and this is the residual strength of the clay.

An interesting test that is sometimes conducted in the field in conjunction with permeability tests is hydraulic fracturing. It has been used for years to determine in-situ earth pressures. Such a test is

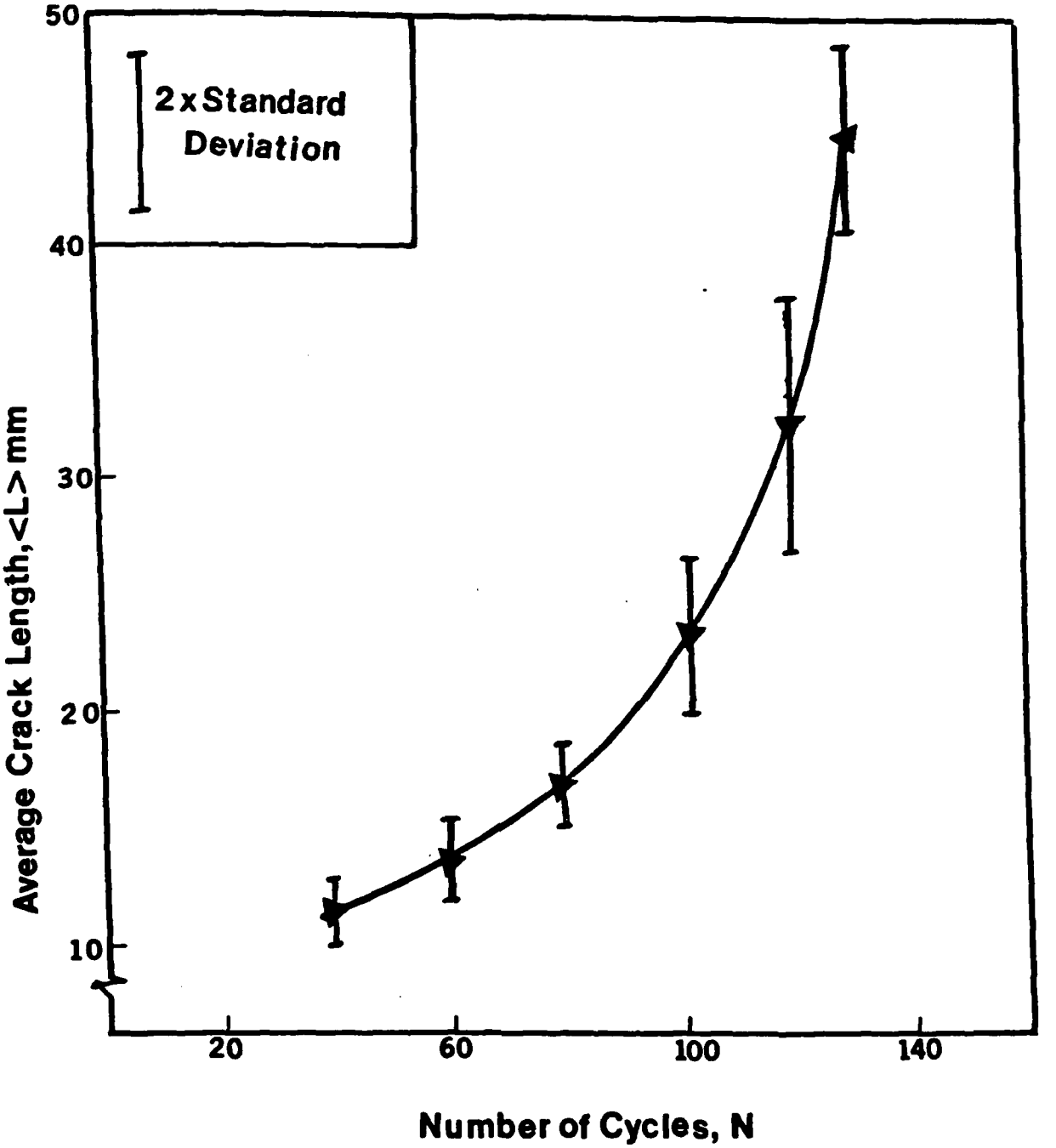

FIG. 16 Average Value of Crack Length and Data Scatter

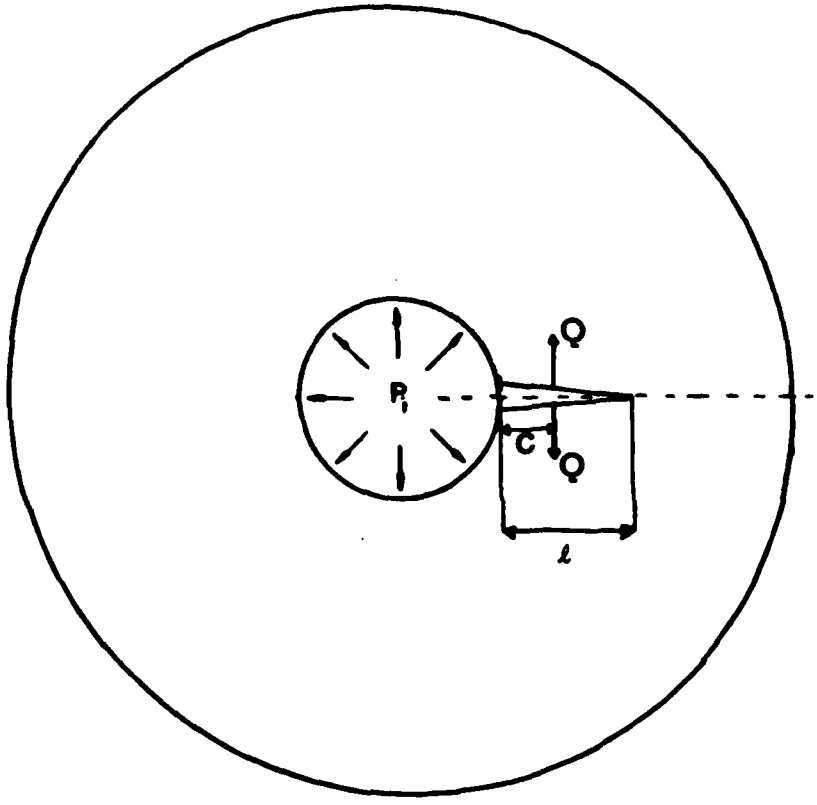

FIG. 17 Derivation of Crack Opening Displacement

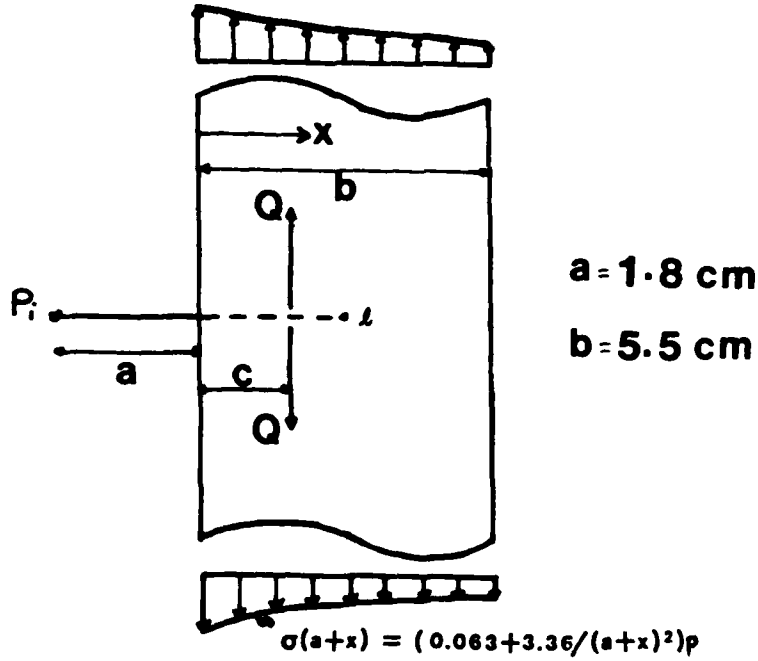

$\sigma(a+x) = (0.063+3.36/(a+x)^2)p$

FIG. 18 The Use of Tada's Strip to Derive an Approximate Solution

disk, we apply the fictitious forces Q then differentiate Π for Q = 0. Since $\Pi_{\text{no crack}}$ does not depend on Q, then

$$\left(\frac{\partial \Pi}{\partial Q}\right)_{Q=0} = \left(-\int_o^{\ell} \frac{\partial^2 \Pi}{\partial \ell \partial Q}\, d\ell\right)_{Q=0} \tag{9}$$

Therefore

$$\left(\frac{\partial \Pi}{\partial Q}\right)_{Q=0} = \left(\frac{1-\nu^2}{E} \int_o^{\ell} \frac{\partial (K_p + K_Q)^2}{\partial Q}\, d\ell\right)_{Q=0} \tag{10}$$

where K_p is the stress intensity factor due to internal pressure without Q and K_Q is the stress intensity factor for Q alone.

Thus,

$$\delta = \left(\frac{2(1-\nu^2)}{E} \int_c^{\ell} K_p \cdot K_Q\, d\ell\right)_{Q=1} \tag{11}$$

Here again, using Green's function for a strip given by Tada [17] we have (Fig. 18)

$$K_p = \int_o^{\ell} \frac{2}{\sqrt{\pi \ell}} \sigma(a+x)\, F\left(\frac{x}{\ell}, \frac{\ell}{w}\right) dx = K_p\left(p, \ell, \frac{\ell}{w}\right) \tag{12}$$

$$K_Q = \frac{2Q}{\sqrt{\pi \ell}} F\left(\frac{c}{\ell}, \frac{\ell}{w}\right) \tag{13}$$

$$\delta = \frac{2(1-\nu^2)}{E} \int_c^{\ell} K_p\left(p, x, \frac{x}{w}\right) \cdot K_Q\left(\frac{c}{x}, \frac{x}{w}\right) dx \tag{14}$$

Eq. 14 was numerically integrated and the results shown in Fig. 19. Crack opening displacements (COD) are measured at the tip of the notch which is 10mm from the inside edge of the disk. Fig. 20 shows the COD for four tests versus the number of cycles, and Fig. 21 the average of those tests and the

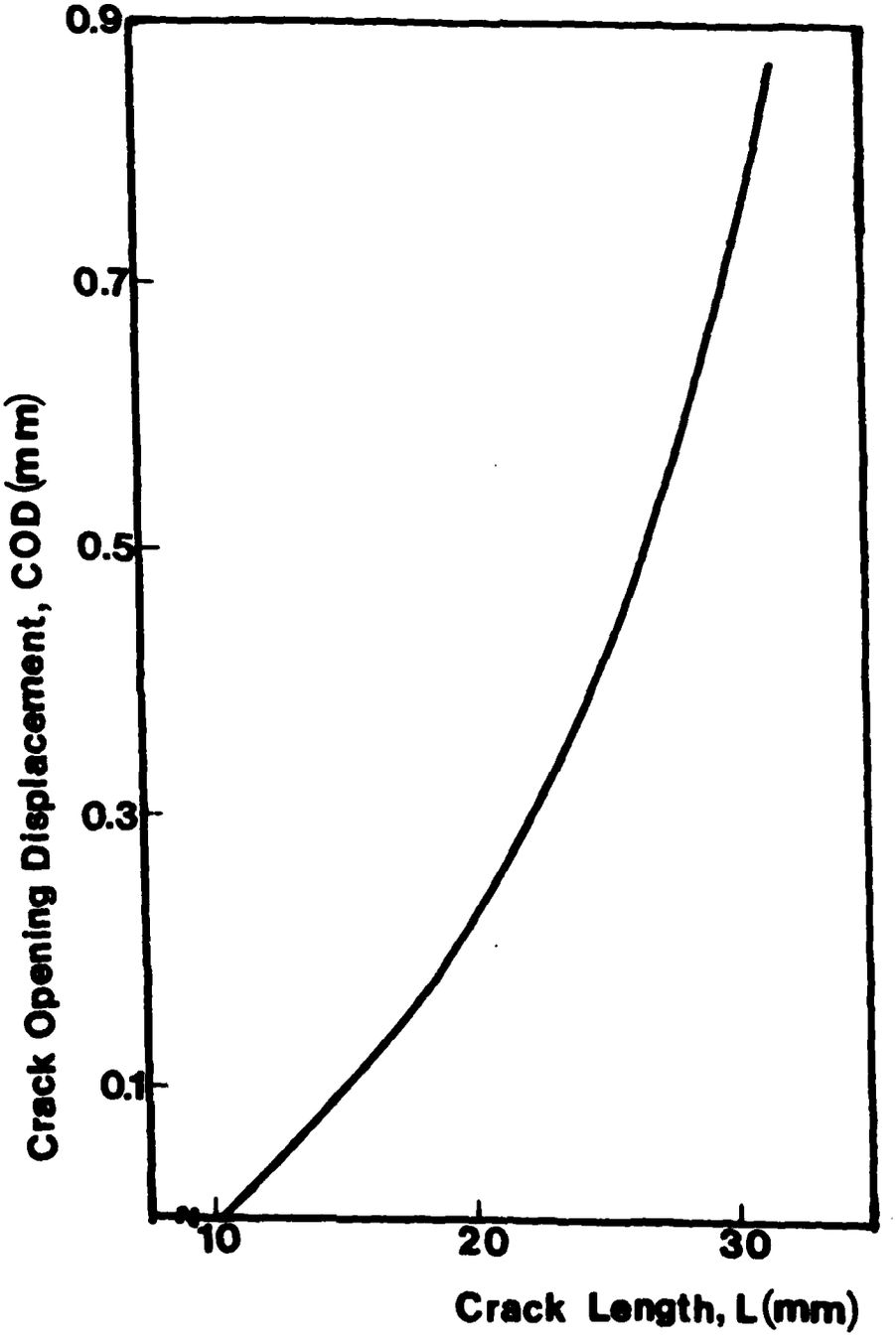

FIG. 19 Calculated Values of the COD Versus ℓ

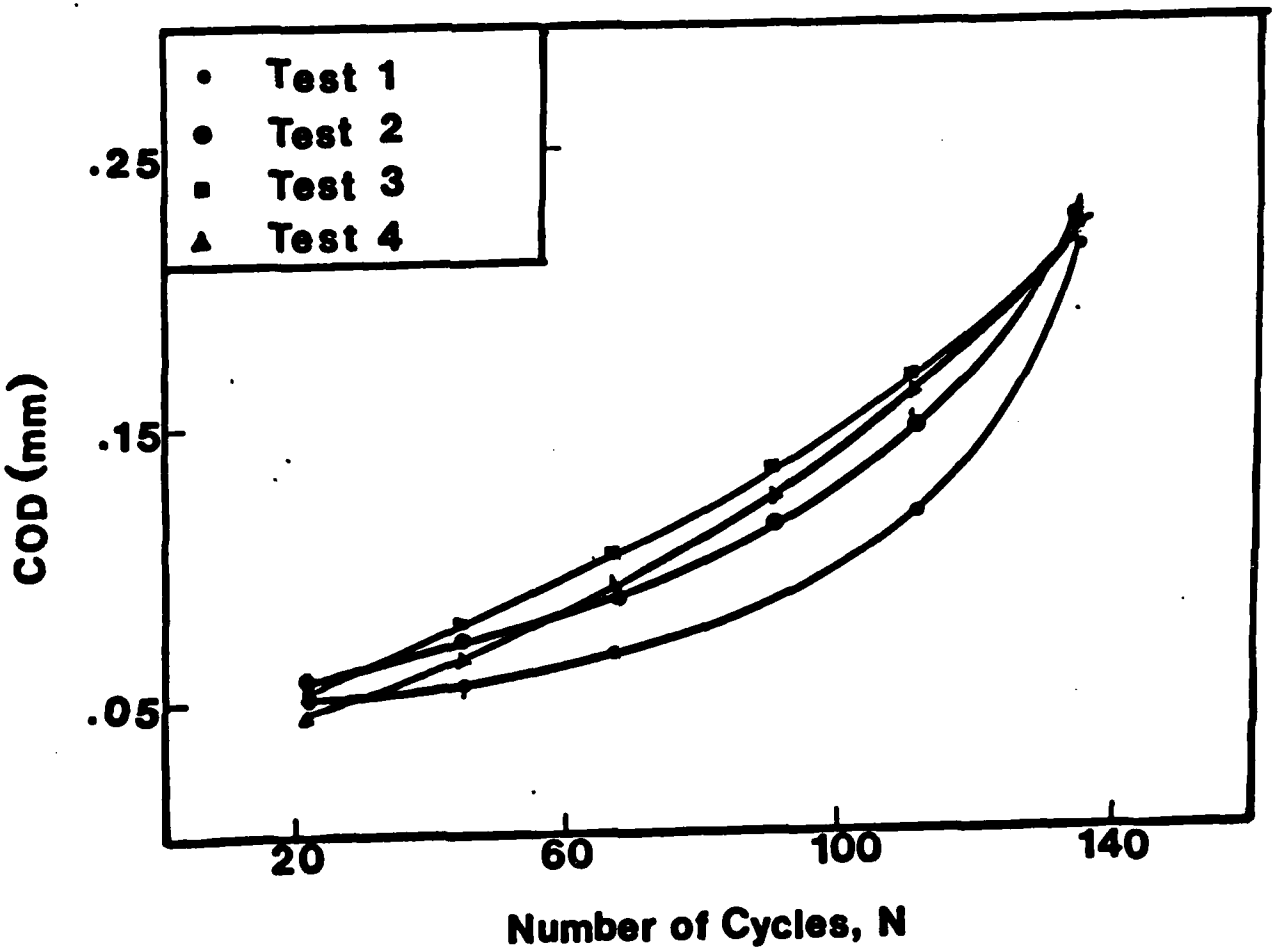

FIG. 20 Measured Values of the COD Versus N

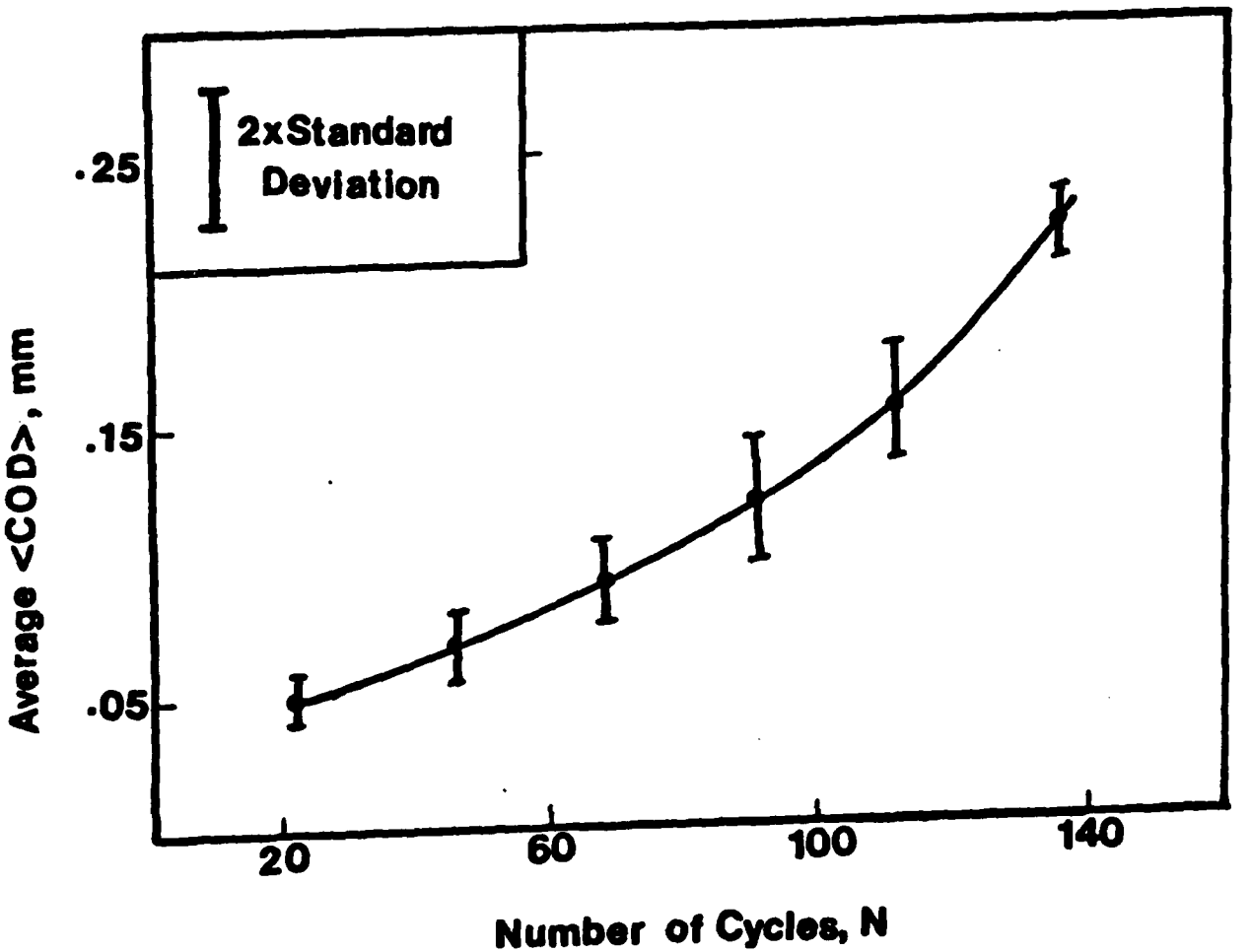

FIG. 21 Average Values of the COD Versus N

scatter involved. Combining figures 19, 20 and 21 one can deduce the relation between the crack length and the number of cycles. This relation is shown in Fig. 22, together with the experimentally measured one. The two curves are signficantly different. This may be due to the fact that the COD versus the crack length was obtained from a strip instead of from a disk. Apparently the error due to such an approximation increases with the crack length. Also linear elasticity may have limited applicability to the material. Both these limitations can be eliminated by further theoretical developments. In addtiion the experimental length of the crack was obtained from outside observation on the face of the disk. Cross sections would help insure that this length indeed extends throughout the thickness.

The kinetics of crack propagation in terms of crack propagation rate versus crack length obtained from direct observation is shown in Fig. 23. The relation between $\frac{d\ell}{dN}$ and ℓ strongly depends on the specimen's geometry and thus does not represent a material behavior. The same time, the energy release rate J accounting for specimen geometry, crack length and loading conditions is commonly used as an invariant parameter. Fig. 24 shows the energy release rate versus the crack length. $\frac{d\ell}{dN}$ versus J is then plotted in Fig. 25. This last relation, if verified in further experiments, is at the core of the development of constitutive equations for crack propagation.

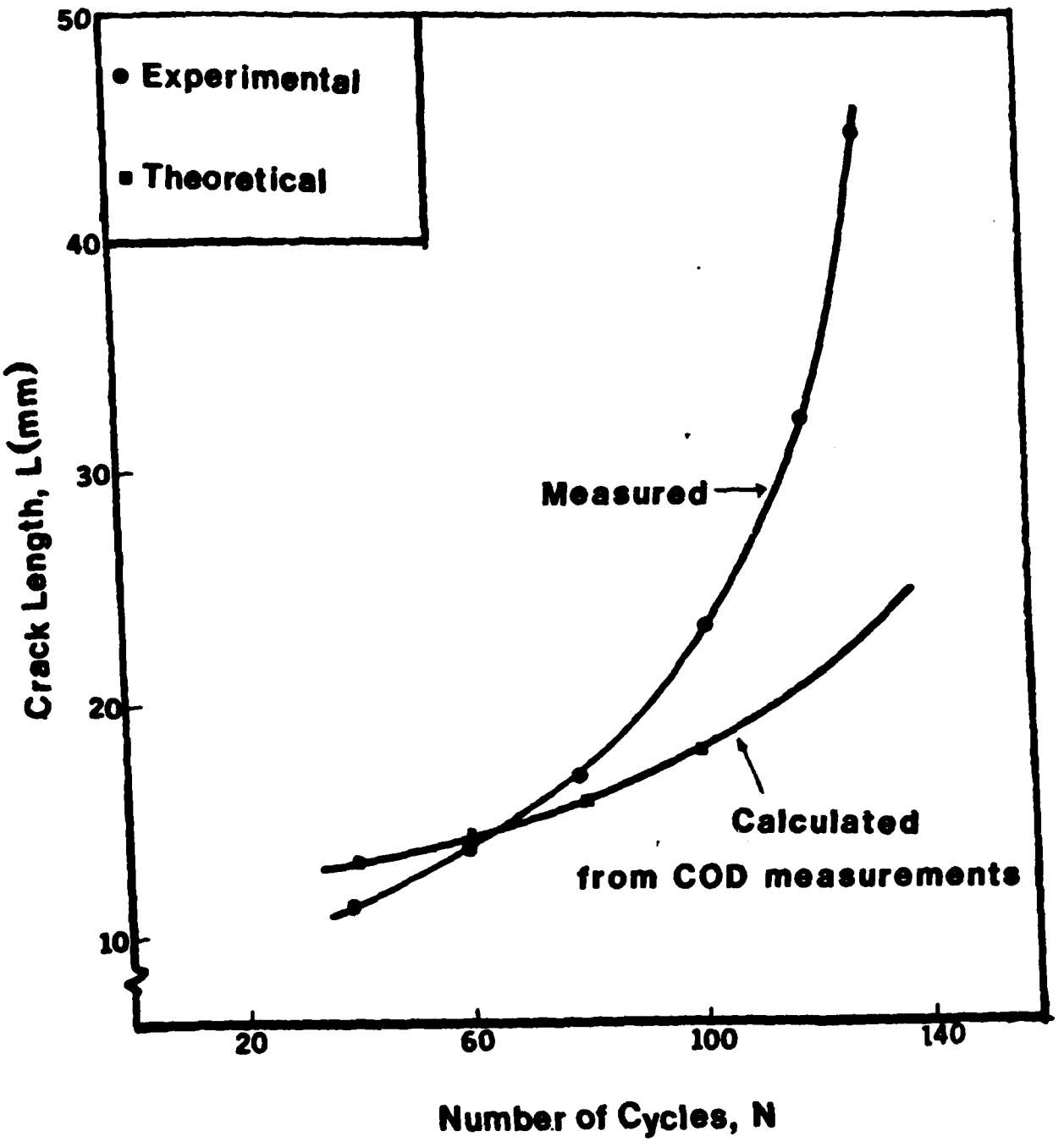

FIG. 22 Comparison Between Measured and Calculated Crack Lengths

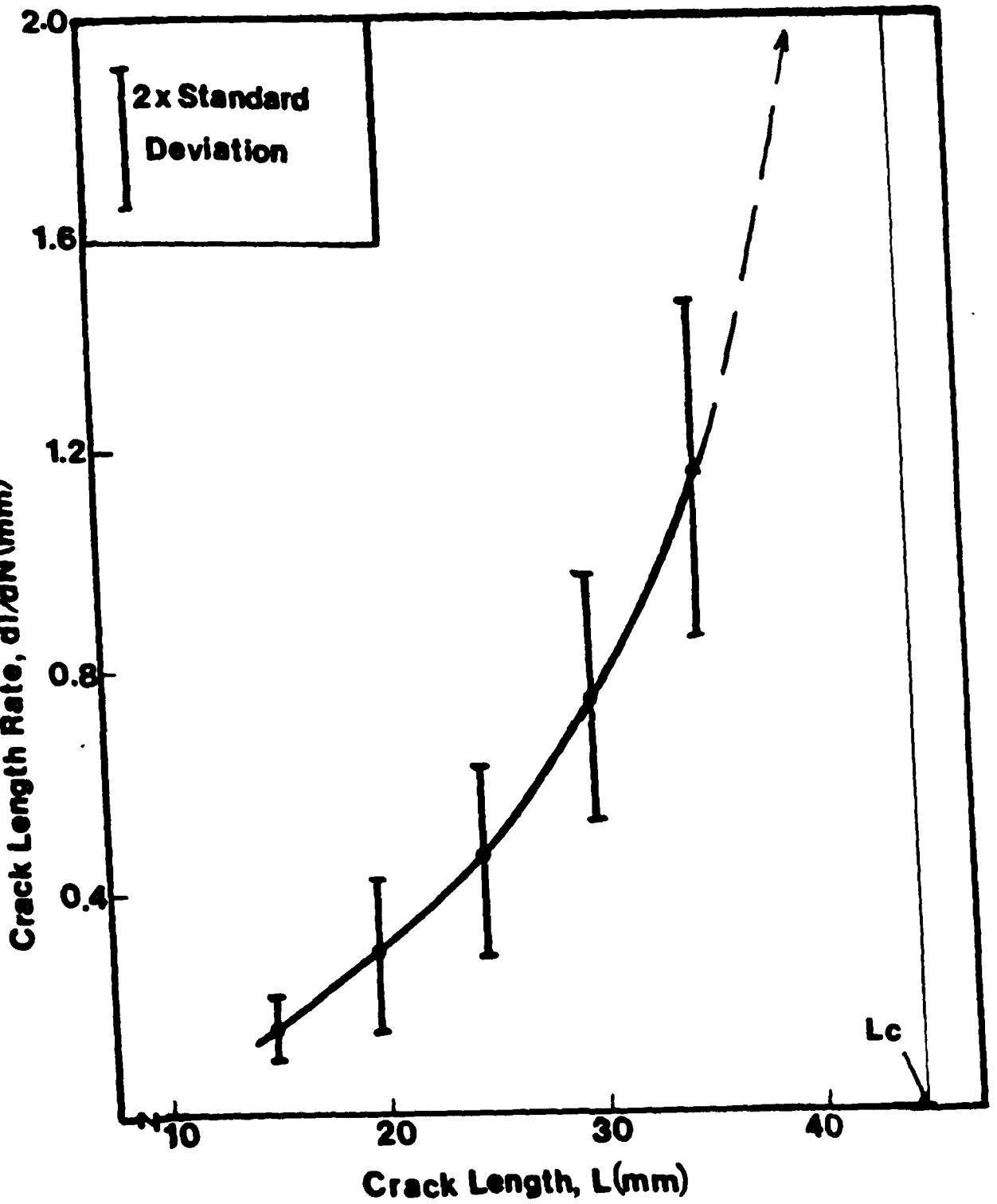

FIG. 23 Crack Length Rate Versus L

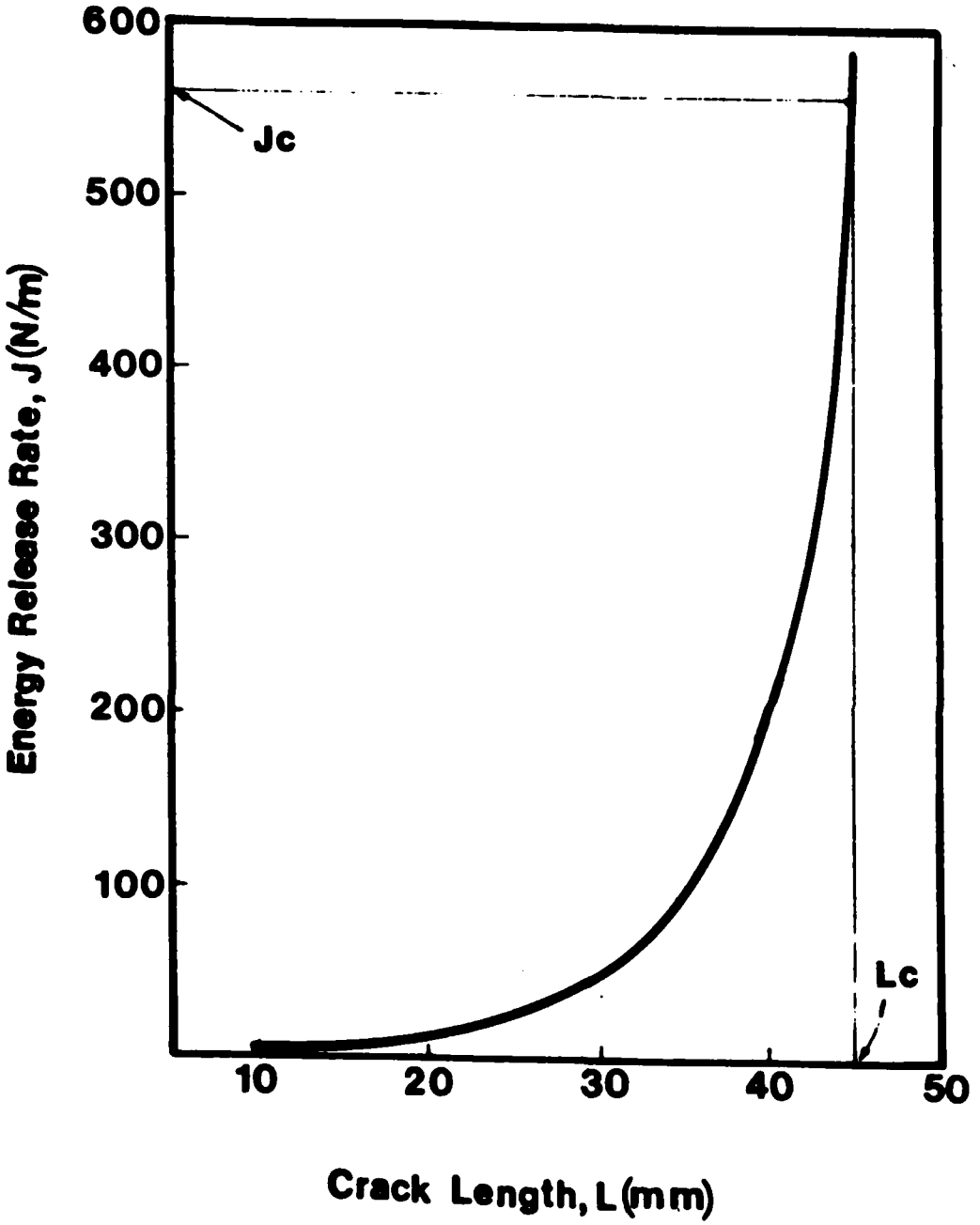

FIG. 24 Energy Release Rate Versus L

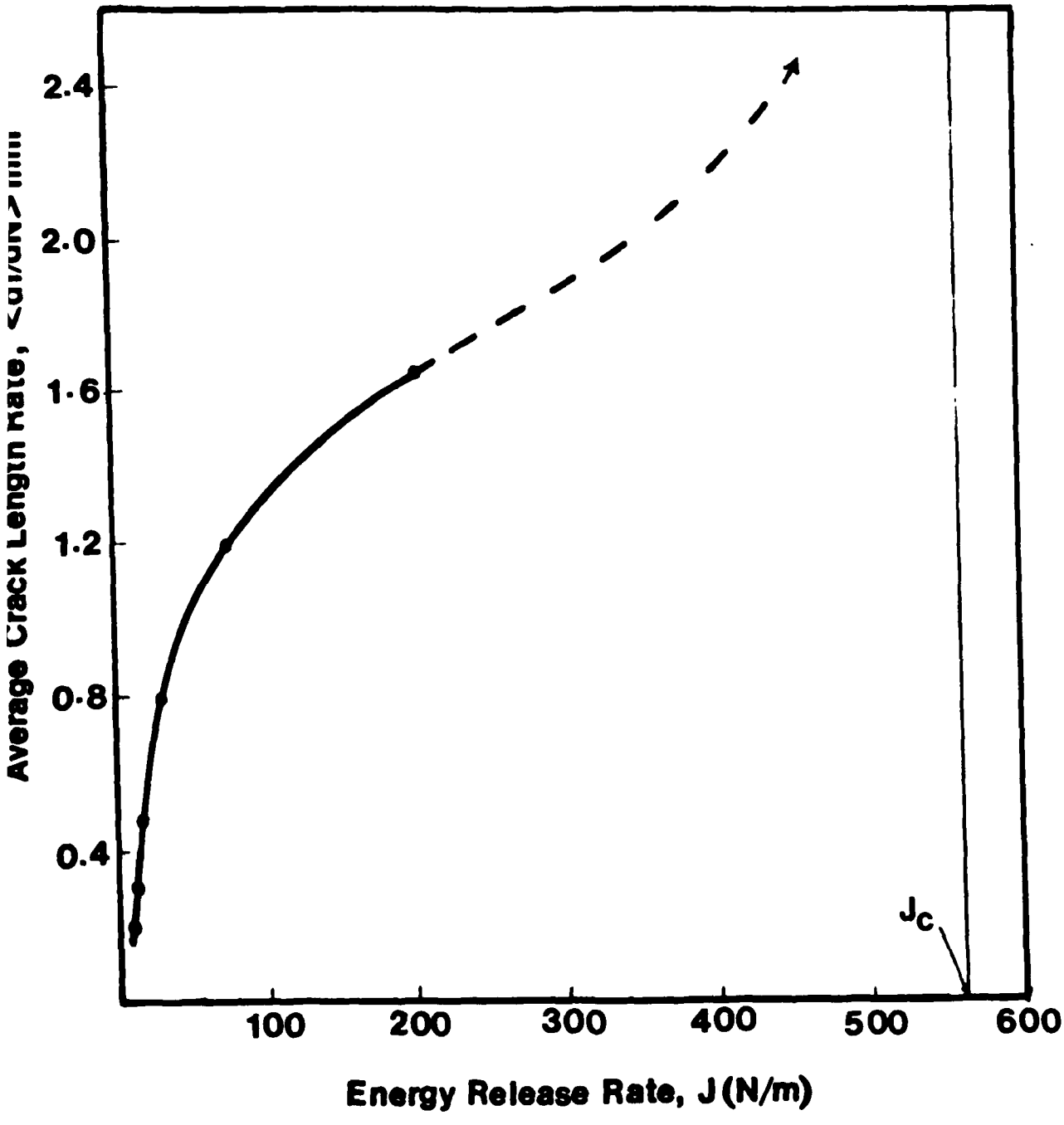

FIG. 25 Average Crack Length Rate Versus Energy Release Rate

PART III: DETERMINATION OF THE CRITICAL VALUE OF THE STRESS INTENSITY FACTOR K_{IIC} FOR MODE II FRACTURE

In this mode the displacement of the crack surfaces is parallel to the plane of the crack. the sample configuration used is that of a thin long hollow cylinder with the dimensions shown in Fig. 26. Once the length of the crack and the critical shearing stress are known a solution due to Erdogan and Ratwani [6] allows one to compute K_{IIC}.

IIIa - Sample Preparation and Testing Equipment

Clay slurries consolidated at approximately 280 kPa were first cut in a shape of a hollow cylinder. A special lathe was used to reduce them to the size shown in Fig. 26. Two diametrically opposite horizontal notches were cut in the specimens and 2 layers of teflon tape inserted in them to prevent hydrostatic pressure from closing and healing the crack. The specimens were then placed in a special cell where they were one dimensionally consolidated under a given cell pressure. Three cell pressures were used leading to vertical consolidation pressures of 1394, 1174 and 954 kPa; K_o for this clay being 0.47. The samples were then allowed to rebound at a cell pressure of 207 kPa leading to vertical overconsolidation ratios of 6.7, 5.7 and 4.6.

A system of pullies and actuator was used to apply rapidly a very high torque to the piston; while transducers inside the cell measured the actual torque transmitted to the sample, and the angle of rotation. These values were recorded on an X-Y plotter. The maximum torque is the critical value needed to compute K_{IIC}. Fig. 26 shows a series of failure surfaces in MODE II for 3 of the hollow cylinders tested. Fig. 27 shows the torsional set up

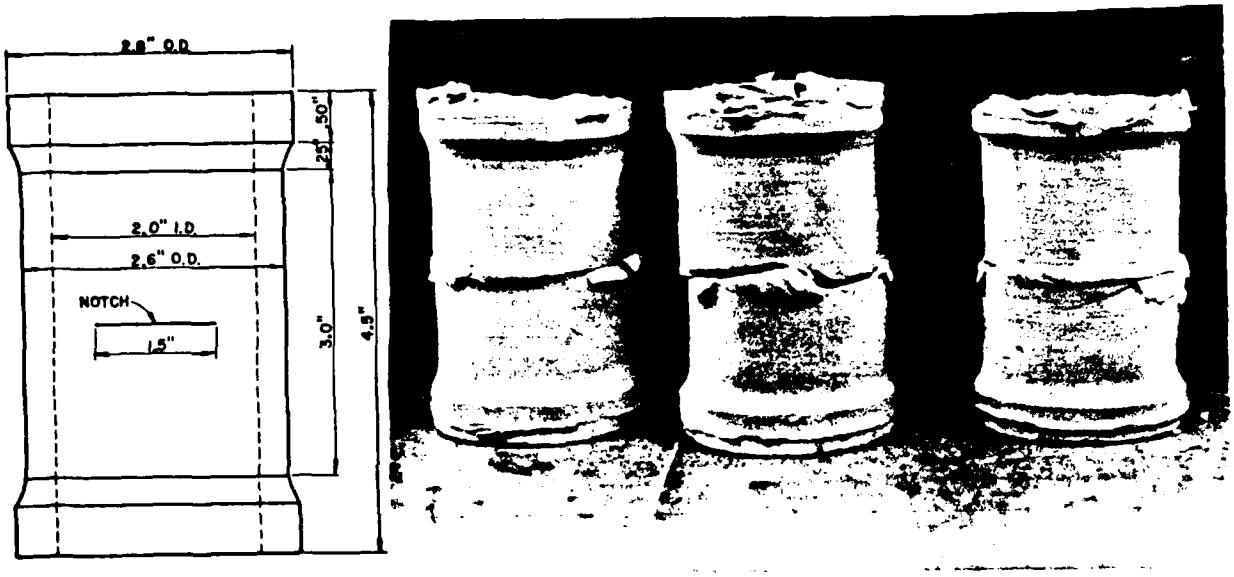

FIG. 26 Failure of Hollow Cylinder in Mode II

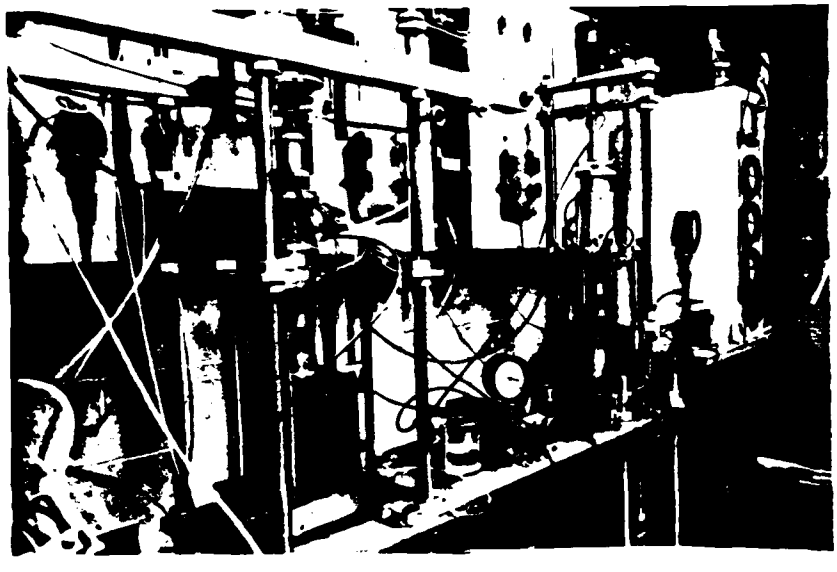

FIG. 27 Mode II Torsional Testing System

th the hollow cylinders of clay inside pressurized cells.

IIb - Calculation of K_{IIC}

Knowing the geometry of the sample and the crack as well as the ritical torque, Erdogan's [6] solution yields the value of K_{IIC}. Fig. 28 nows the relation between K_{IIC} and the overconsolidation ratio for the aolinite tested.

IIc - Observations of Damaged Zones in the Vicinity of Cracks

One of the most intriguing observations made during the study is elated to the changes in the material micro-structure caused by crack ropagation. It is well known that right on the fracture (or slip) surface he clay particles align themselves parallel to this surface. However, eyond this exceedingly thin layer made of the thickness of a few articles, a zone of damage is present. To examine this zone of damage a large portion of the hollow cylinder surrounding the crack was first vacuum mpregnated with wax. Then a section of about 1 cm in height was cut erpendicular to the fracture surface with a diamond tipped wafering blade (Fig. 29). When photographed in the direction indicated by the arrow, Fig. 30 is obtained. The magnification in Fig. 30 is approximately 10, which is very small compared to what is ususally obtained in the scanning electron microscope. The advantage of such a magnification is that one can see the overall picture of the damage and the zone involved.

In Fig. 30, a damage zone similar in shape to the zone predicted by plasticity theory can be seen. However, contrary to plasticity which involves a field of slip or Luder lines, this zone consists of a honeycombed network of fissures (dark regions) enclosing undamaged material (light regions). the cellular structure of this region is quite evident

PART IV: BIBLIOGRAPHY

1. Bishop , A.W. (1967). Discussion on Shear Strength of Stiff Clay. Proc. Geotechnical Conf., Oslo 2, 142-150.

2. Bishop, A.W. & Little, A.L. (1976). The Influence of the Size and Orientation of the Sample on the Apparent Strength of the London Clay at Maldon, Essex. Proc. Geotechnical Conf., Oslo 1, 89-96.

3. Bjerrum, L. (1967). Progressive Failure in slopes of Over-Consolidated Plastic Clay and Clay Shales. J. Soil Mech. Fdns. Div. Am. Soc. Civ. Engrs. 93, SM5, Part I.

4. Bjerrum, L. (1966). Secondary Settlement of Structures Subjected to Large Variations in Live Load - in Rheology and Soil Mechanics, Ed. by J. Kravtchenko and P. Sirieys, Springer, Berlin.

5. Chudnovsky, A. (1983). Crack Layer Theory, NASA Report, Grant NAG-3-23.

6. Erdogan, F.E. and Ratwani, M. (1973). A Circumferential Crack in a Cylindrical Shell Under Torsion. Int. J. Fract. Mech., 8, 87-95.

7. Fookes, P.G. (1965). Orientation of Fissures in Stiff Overconsolidated Clay of the Siwalik System. Geotechnique 15, No. 2, 195-206.

8. Lo, K.Y. Adams, J.I. & Seychuk, J.L. (1969). The Shear Behaviour of a Stiff Fissured Clay. Proc. 7th Int. Conf. Soil Mech., Mexico 1, 249-255.

9. Lo, K.Y. (1970). The Operational Strength of Fissured Clay. Geotechnique 20, No. 1, 57-74.

10. Morgenstern, N.R. (1967). Shear Strength of Stiff Clays. Proc. Geotechnical Conf., Oslo 2, 59-69.

11. Morgenstern, N.R. & Tchalenko, J.S. (1967). Microstructural Observations on Shear Zones From Slips in Natural Clays. Proc. Geotechnical Conf., Oslo 1, 147-152.

12. P. Glansdorff and I. Prigogine (1971). Thermodynamic Theory of Structure, Stability and fluctuations". Wiley-Interscience. New York.

13. Simons, N.E. (1967). Discussion on Shear Strength of Stiff Clay. Proc. Geotechnical Conf., Oslo 2, 159-160.

14. Skempton, A.W. (1966). Some Observations on Tectonic Shear Zones. proc. 1st. International Conference on Rock Mechanics (Libson) Vol. 1,

PART IV: CONCLUSION

A framework for the use of fracture mechanics in the study of the behavior of stiff clays has been established. Tests have been proposed and then conducted for the determination of K_{IC} and K_{IIC}. The kinetics of crack propagation in Mode I has been examined. Experimentally this is the first time a pure Mode II has been obtained for any material; and the observations made on the microstructure in the damage zone seem to provide a turning point in the interpretation of failure phenomena in clays.

Perhaps the most important contribution of K. Terzaghi to soil mechanics was his bringing together in one treatise many of the branches of the mechanics of continuous media; and casting them in a form easily used by engineers. Fracture mechanics is a relatively young science which has its place in the interpretation of the behavior of soil masses. It is hoped that this research will help develop new testing and analysis techniques leading to more rational design in fissured soils.

TABLE I

Critical length of cracks for various h and i.

h \ i°	15.00	20.00	25.00	30.00	35.00
5.0	33.13	20.05	14.11	11.04	9.38
6.0	23.01	13.92	9.80	7.67	6.51
8.0	12.94	7.83	5.51	4.31	3.66
10.0	8.28	5.01	3.53	2.76	2.34

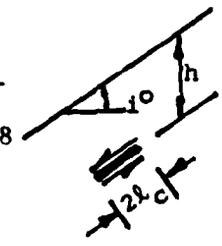

Conventionally the energy release rate for plane strain and MODE II is written $J_1 = (1 - \nu^2)K_{II}^2/E$, where E and ν are Young's modulus and Poisson's ratio respectively. Thus,

$$\frac{\partial J_1}{\partial \ell} = \frac{2(1 - \nu^2)}{E} K_{II} \frac{\partial K_{II}}{\partial \ell} > 0 \tag{23}$$

and condition (21b) is always satisfied. Condition (22) can be rewritten in the following equivalent form

$$K_{IIS} = K_{IIC} \tag{24}$$

where K_{IIC} is the fracture toughness coefficient. It can be obtained for instance from tests conducted on hollow cylinders in MODE II fracture. Substituting (22) into (24) we obtain the expression for the critical crack length $2\ell_c$. Thus,

$$2\ell_c = \frac{8K_{IIC}^2}{\pi(\rho g h \sin 2i)^2} \tag{25}$$

The values of K_{IIC} for a range of overconsolidation ratios can be obtained from Fig. 28. Table 1 gives values of the critical lengths of crack which would cause catastrophic failure for various depths h and slope inclinations i. The value of ρg is 17.3 kN/m^3 and that of K_{IIC} is 156 x 10^3 $Nm^{3/2}$. The dimensions are in meters. As one can notice the results seem to be quite reasonable.

sufficient condition of stability (19) reduces to

$$\left.\frac{\partial J_1}{\partial \ell}\right|_{\substack{\sigma = \text{const} \\ T = \text{const}}} \leq 0 \qquad (20)$$

Therefore, at constant temperture T, the necessary and sufficient conditions of instability are

$$J_1 = \gamma^{eff} \quad (a) \qquad \left.\frac{\partial J_1}{\partial \ell}\right|_{\sigma = \text{const}} > 0 \quad (b) \qquad (21)$$

IVb - Application to the Stability of Infinite Slopes

Consider an infinite slope with a crack of length 2ℓ parallel to the surface and at a depth h. It will be assumed that there is no shearing resistance along the crack and that for saturated overconsolidated undrained clay, compressive stresses do not change the shear response. A MODE II fracture is under consideration. The shearing stress on any plane parallel to the surface at a depth h is given by $\tau = \rho g h \sin(i) \cos(i)$, where i is the inclination of both slope and crack. Let us now consider a MODE II crack in an infinite plane under the uniform shearing stress and use the principle of superposition. If K_{II_∞} is the fracture toughness of the plane and K_{IIS} is that of the problem at hand then $K_{IIS} = K_{II_\infty}$ because of the symmetries involved in an infinite slope. Thus,

$$K_{II_\infty} = K_{IIS} = \tau\sqrt{\pi\ell} = \frac{1}{2}\rho g h \sqrt{\pi\ell} \sin(2\, i) \qquad (22)$$

appears as a generalized force reciprocal to the generalized flux $\dot{\ell}$.

When $(\gamma^* R_1 - J_1) \leq 0$ the crack propagates spontaneously. When $(\gamma^* R_1 - J_1) > 0$, the crack can prorpagate only if $\dot{D} \geq \dot{\ell}(\gamma^* R_1 - J_1)$, i.e., if the dissipation compensates for the negative entropy production $\dot{\ell}(J_1 - \gamma^* R_1)$. This implies that the crack propagation is controlled by dissipative processes like irreversible deformation, diffusion, chemical reaction, etc. Apparently, the critical condition for instability (stability) is

$$J_1 - \gamma^* R_1 = 0 \tag{17}$$

which is Griffith's criterion if $\gamma^* R_1$ is taken as the surface energy. This quantity in the fracture mechanics literature is referred to as γ^{eff} or the critical energy release rate J_{1C}. While Eq. 17 is a necessary condition for instability, the sufficient condition results from the universal criterion of evolution. For a stable process, the following inequality holds [12]:

$$\frac{d\dot{S}_i}{dt} = \sum_k j_k \frac{dX_k}{dt} \leq 0 \tag{18}$$

where j_k is assumed to remain constant. For an elastic crack $\dot{D} = 0$ and Eqs. 16 and 18 yield

$$T\frac{d\dot{S}_i}{dt} = \dot{\ell}^2 \left.\frac{\partial(J_1 - \gamma^* R_1)}{\partial \ell}\right|_{\substack{\sigma = \text{const} \\ T = \text{const}}} \leq 0 \tag{19}$$

where σ is the stress tensor. If the damaged zone does not change as the crack length increases one can assume that $\gamma^* R_1 = \gamma^{eff}$ is constant. The

PART IV: THERMODYNAMIC CRITERIA OF STABILITY AND APPLICATION TO THE SLOPE STABILITY PROBLEM

IVa - Thermodynamic Criteria of Stability

For an irreversible process the second law of thermodynamics states that the rate of entropy production $\dot{S}_i$ is such that

$$\dot{S}_i = \sum_k j_k X_k \geq 0, \tag{15}$$

where j_k is a generalized flux and X_k is a generalized force. The rate of entropy production for a propagating crack has be written by Chudnovsky (5)

$$T\dot{S}_i = \dot{D} + \dot{\ell}(J_1 - \gamma^* R_1) \geq 0 \tag{16}$$

where, T is the absolute temperature, D is the portion of the irreversible work spent on the development of micro damage in the vicinity of the crack tip, $\dot{\ell}$ is the rate of crack growth; $J_1 = -\frac{d\Pi}{d\ell}$ is the energy release rate, Π is the potential energy also called Gibbs potential; γ^* is the specific enthalpy of damage. It can be looked upon as the surface energy if the damage consists of microcracks only. R_1 is a value integral characterizing the damaged zone around the crack tip [5]. Whereas $\gamma^* R_1$ represents the amount of energy needed for the crack and its surrounding damaged zone to advance, J_1 characterizes the amount of accumulated potential energy available for crack propagation. Thus $(\gamma^* R_1 - J_1)$ represents the energy barrier which must be overcome for the crack to advance. Within the framework of irreversible thermodynamics, $(J_1 - \gamma^* R_1)$

in the enlargements of Fig. 31.

In addition to this damage zone Fig. 30 shows several localized bands of discontinuity of slippage. Enlargements of one of these localized discontinuities is shown in Fig. 32. The localized discontinuity has a cellular structure similar to the honeycomb damage zone, but on a much smaller scale. These localized discontinuities are inclined cracks which have propagated from the notch tip as shown in Fig. 33. The horizontal crack, rather than the inclined cracks, led to catastrophic failure.

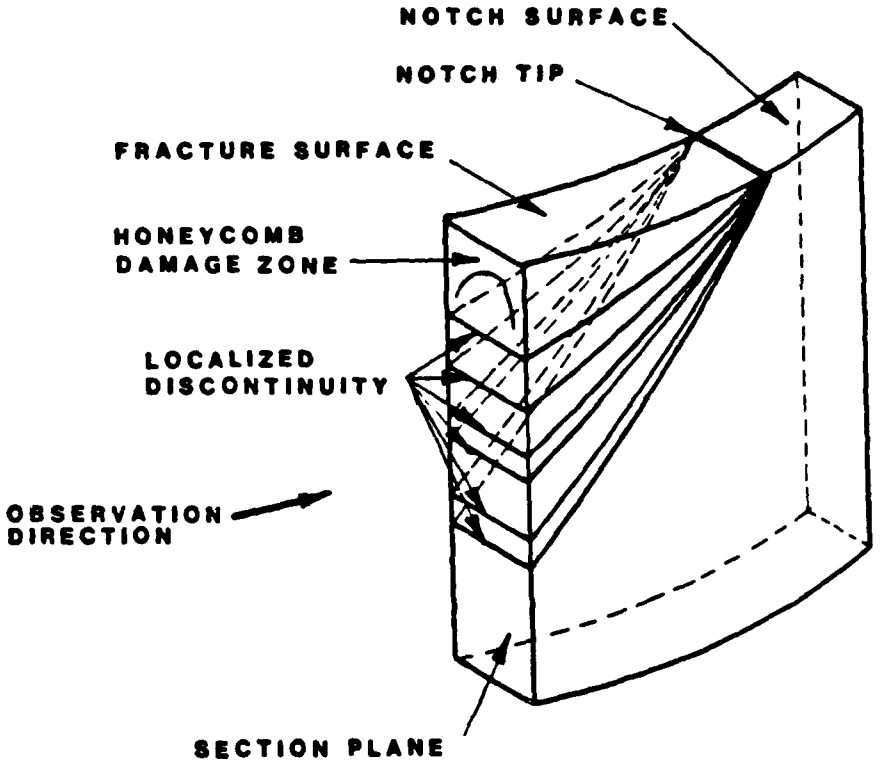

FIG. 33 Fracture Surface and Damage Zones.

FRAGMENTS OF LOCALIZED DISCONTINUITY

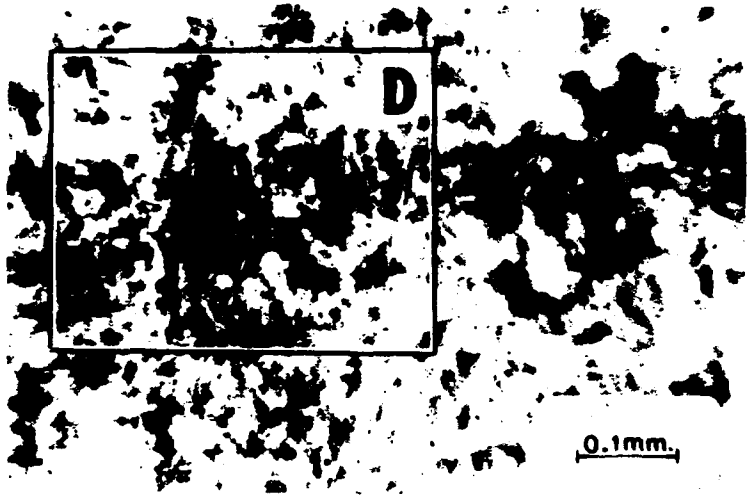

B

D

FIG. 32 Fragments of Localized Discontinuity

FRAGMENTS OF HONEYCOMB DAMAGE

A

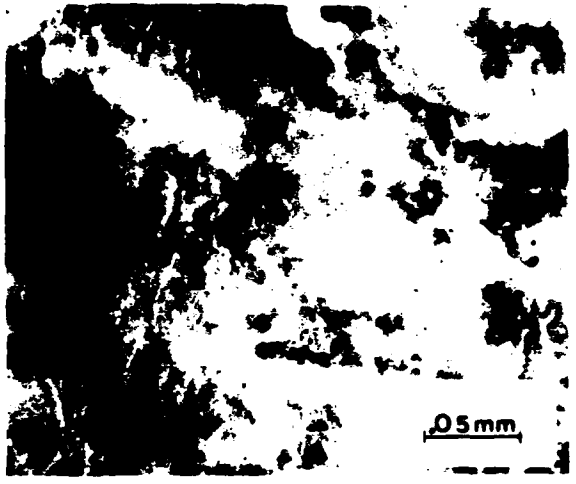

C

FIG. 31 Fragments of Honeycomb Damage

FRAGMENTS OF HONEYCOMB DAMAGE

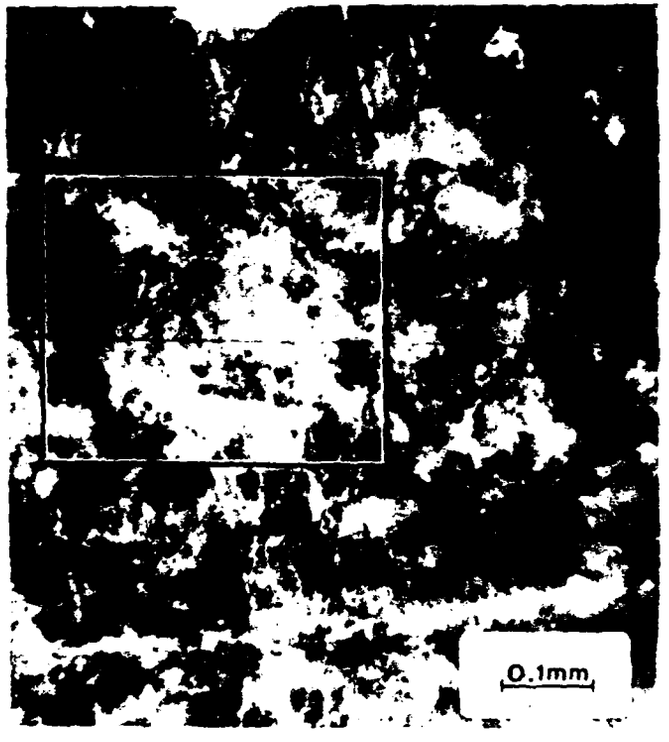

A

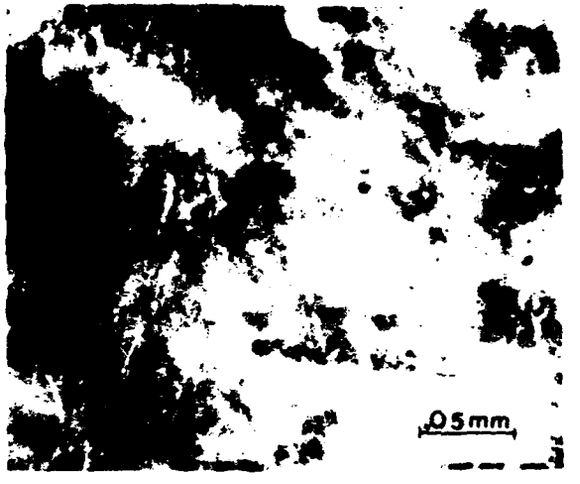

C

FIG. 31 Fragments of Honeycomb Damage

DAMAGE PATTERN

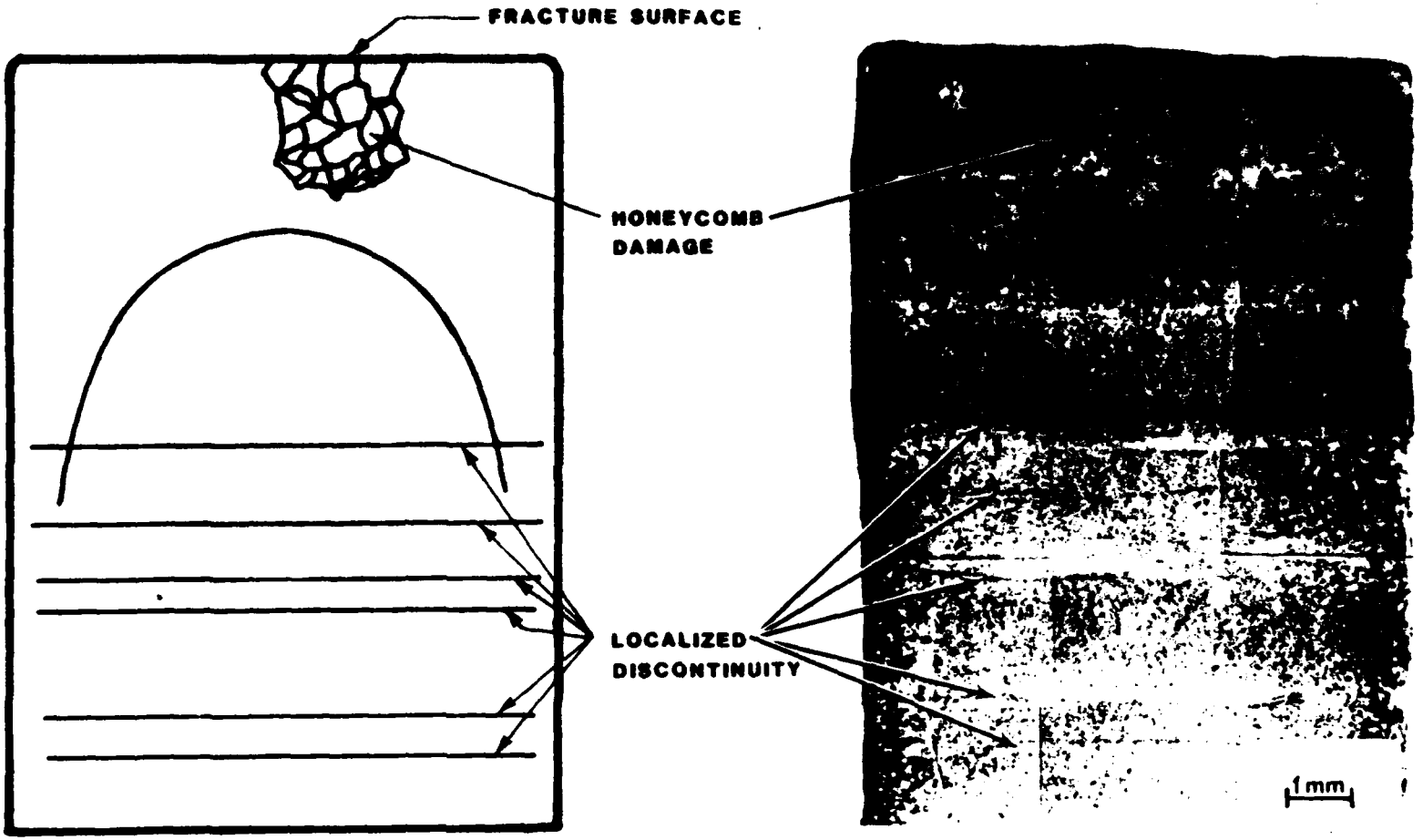

FIG. 30 Damaged Pattern and Localized Discontinuities

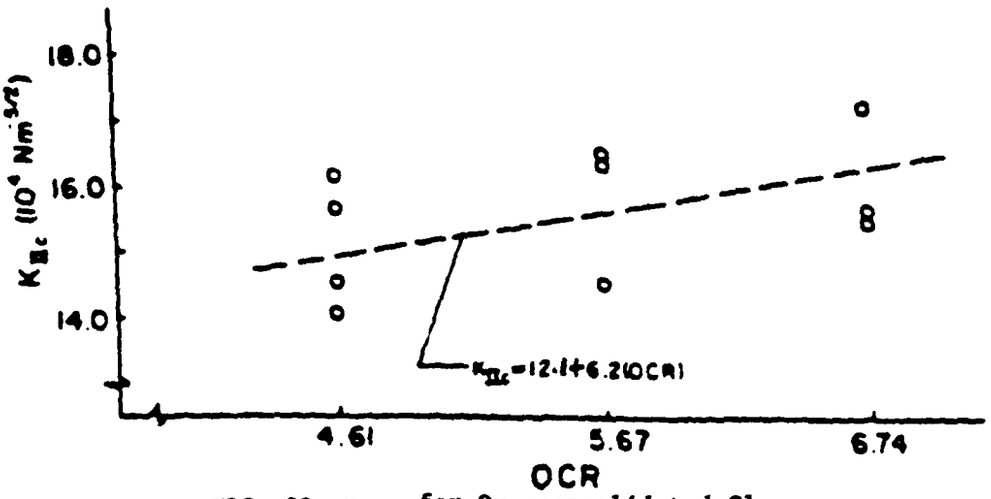

FIG. 28 K_{IIC} for Overconsolidated Clay

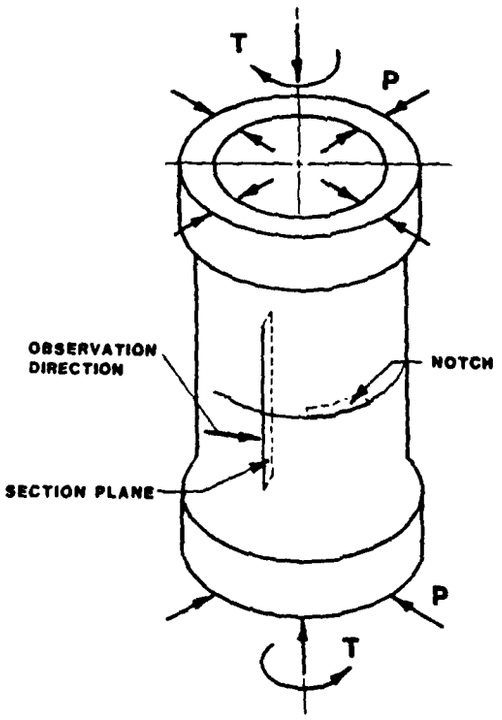

FIG. 29 Sections Observed in Mode II Specimen Fracture

pp. 329-335.

15. Skempton, A.W. & Petley, D.J. (1967). The Strength Along Structural Discontinuities in Stiff Clays. Proc. Geotechnical Conf., Oslo 2, 29-46.

16. Skempton, A.W., Schuster, R.L. & Petley, D.J. (1969). Joints and Fissures in the London Clay at Wraysbury and Edgware. Geotechnique 19, No. 2 205-217.

17. Tada, H., Paris, P.C. and Irwin, G.R. (1973). The Stress Analyses of Cracks Handbook. Del Research Corporation 2-27.

18. Yong, R.N., and Warkentin, B.P. (1975). Soil Properties and Behavior Elsevier, New York.

END

FILMED

5-85

DTIC